



UNIVERSITÀ  
DEGLI STUDI  
FIRENZE

## FLORE

# Repository istituzionale dell'Università degli Studi di Firenze

### **Antifibrogenic effects of canrenone, an antialdosteronic drug, on human hepatic stellate cells**

Questa è la Versione finale referata (Post print/Accepted manuscript) della seguente pubblicazione:

*Original Citation:*

Antifibrogenic effects of canrenone, an antialdosteronic drug, on human hepatic stellate cells / CALIGIURI A.; DE FRANCO R. M. S.; ROMANELLI R. G.; GENTILINI A.; MEUCCI M.; P. FAILLI; MAZZETTI L.; ROMBOUTS K.; GEERTS A; VANASIA M.; GENTILINI P.; MARRA F.; PINZANI M.. - In: GASTROENTEROLOGY. - ISSN 0016-5085. - ELETTRONICO. - 124:(2003), pp. 504-520.

*Availability:*

This version is available at: 2158/208607 since:

*Publisher:*

W B Saunders Company:Fulfillment Department, The Curtis Center, Independence Square West:

*Terms of use:*

Open Access

La pubblicazione è resa disponibile sotto le norme e i termini della licenza di deposito, secondo quanto stabilito dalla Policy per l'accesso aperto dell'Università degli Studi di Firenze (<https://www.sba.unifi.it/upload/policy-oa-2016-1.pdf>)

*Publisher copyright claim:*

(Article begins on next page)

## Antifibrogenic Effects of Canrenone, an Antialdosteronic Drug, on Human Hepatic Stellate Cells

ALESSANDRA CALIGIURI,\* RAFFAELLA M. S. DE FRANCO,\* ROBERTO G. ROMANELLI,\*  
 ALESSANDRA GENTILINI,\* MARTA MEUCCI,\* PAOLA FAILLI,† LUCA MAZZETTI,†  
 KRISTA ROMBOUITS,§ ALBERT GEERTS,§ MASSIMO VANASIA,||  
 PAOLO GENTILINI,\* FABIO MARRA,\* and MASSIMO PINZANI\*

\*Dipartimento di Medicina Interna and †Dipartimento di Farmacologia Clinica e Preclinica, Università di Firenze, Firenze, Italy; §Laboratory for Molecular Liver Cell Biology, Free University of Brussels, Brussels, Belgium; and ||Gienne Pharma S.p.A., Milan, Italy

**Background & Aims:** Several lines of evidence indicate that aldosterone antagonists may exert direct antifibrogenic effects. The aim of this study was to evaluate the possible direct antifibrogenic effects of canrenone, the active metabolite of spironolactone, in activated human hepatic stellate cells. **Methods:** The effects of canrenone were assessed on platelet-derived growth factor-induced mitogenic and chemotactic effects and the increased de novo synthesis of different extracellular matrix components induced by transforming growth factor- $\beta$ 1. **Results:** Canrenone dose-dependently reduced platelet-derived growth factor-induced cell proliferation and motility. This effect was not associated with either changes in the phosphorylation of platelet-derived growth factor receptor and phospholipase C  $\gamma$  or in the activation of the Ras/extracellular signal-regulated kinase pathway, whereas it was accompanied by a dose-dependent inhibition of platelet-derived growth factor-induced phosphatidylinositol 3-kinase activity. In addition, canrenone inhibited the activity of the Na<sup>+</sup>/H<sup>+</sup> exchanger 1 induced by platelet-derived growth factor. The effect of canrenone on Na<sup>+</sup>/H<sup>+</sup> exchanger 1 activity was reproduced by phosphatidylinositol 3-kinase inhibitors, thus supporting an inhibitory action of canrenone on phosphatidylinositol 3-kinase activity. To further address this possibility, the action of canrenone was compared with that of 2 established Na<sup>+</sup>/H<sup>+</sup> exchanger 1 inhibitors: ethylisopropylamiloride and cariporide. Whereas ethylisopropylamiloride was able to inhibit platelet-derived growth factor-induced phosphatidylinositol 3-kinase activity, cariporide was without any effect. Both compounds reproduced the effects of canrenone on platelet-derived growth factor-induced mitogenesis and chemotaxis. Finally, canrenone was able to reduce transforming growth factor- $\beta$ 1-induced de novo synthesis of procollagen type I/IV and fibronectin and thrombin-induced hepatic stellate cell contraction. **Conclusions:** These results indicate that canrenone may be active as an antifibrogenic drug.

Antialdosteronic drugs are commonly used as diuretics in the treatment of cirrhotic ascites, alone or in association with loop diuretics. In addition, this class of drugs has been proposed for the treatment of portal hypertension in cirrhotic patients without ascites, and, accordingly, chronic administration of spironolactone has been shown to be effective in decreasing portal pressure in this clinical setting.<sup>1-3</sup> This beneficial effect has been ascribed to a reduction of the expanded blood volume typical of preascitic cirrhosis and early ascitic cirrhosis.<sup>4,5</sup> However, several lines of evidence suggest that the reduction of portal pressure could also be due to direct effects of spironolactone on factors affecting intrahepatic portal circulation. First, spironolactone and its metabolites potassium canrenoate and canrenone have been shown to induce relaxation of isolated rat aorta rings precontracted by different agonists,<sup>6,7</sup> an effect apparently independent of a possible interference with nongenomic effects of aldosterone or activation of potassium channels.<sup>6</sup> A second relevant issue is related to the possible antagonism of this class of drugs toward the putative profibrogenic effect of aldosterone, particularly highlighted within the cardiovascular system.<sup>8</sup> However, the cellular and molecular mechanisms by which aldosterone induces fibrosis are presently unclear. Although initial reports indicated that aldosterone induces transcrip-

**Abbreviations used in this paper:** BCECF, bis-carboxyethylcarboxy-fluorescein; [Ca<sup>2+</sup>]<sub>i</sub>, intracellular free calcium concentration; ECM, extracellular matrix; EGTA, ethylene glycol-bis( $\beta$ -aminoethyl ether)-N,N,N',N'-tetraacetic acid; EIPA, ethylisopropylamiloride; ERK, extracellular signal-regulated kinase; FAK, focal adhesion kinase; [<sup>3</sup>H]TdR, methyl-[<sup>3</sup>H]thymidine; HOE 642, cariporide; HSC, hepatic stellate cells; NHE, Na<sup>+</sup>/H<sup>+</sup> exchanger; PDGF, platelet-derived growth factor; [pH]<sub>i</sub>, intracellular pH concentration; PI 3-K, phosphatidylinositol 3-kinase; PLC, phospholipase C; SDS-PAGE, sodium dodecyl sulfate-polyacrylamide gel electrophoresis; SFIF, serum-free/insulin-free; TGF- $\beta$ 1, transforming growth factor- $\beta$ 1.

© 2003 by the American Gastroenterological Association

0016-5085/03/\$35.00

doi:10.1053/gast.2003.50058

tion of procollagen I messenger RNA and increases collagen I synthesis in rat cardiac fibroblasts,<sup>9,10</sup> other studies could not confirm these findings.<sup>11,12</sup> To further reinforce the concept that aldosterone does not promote, at least directly, tissue fibrosis, recent work by Rombouts et al.,<sup>13</sup> performed in rat cardiac fibroblasts metabolically labeled with [<sup>35</sup>S]methionine/[<sup>35</sup>S]cysteine, has confirmed that this hormone does not affect de novo collagen synthesis at physiological concentrations ( $10^{-8}$  to  $10^{-10}$  mol/L), whereas an inhibitory effect is observed at  $10^{-7}$  mol/L. In addition, the same group of investigators has also shown that aldosterone does not promote de novo collagen synthesis in activated rat hepatic stellate cells (HSC), a cell type that contributes to the progression of liver fibrosis after chronic liver tissue damage<sup>14</sup> and is potentially involved in the genesis of portal hypertension.<sup>15</sup> In aggregate, these observations tend to rule out a direct profibrogenic effect of aldosterone. However, on the basis of the proposed profibrogenic action of aldosterone, some clinically positive effects of spironolactone in patients with chronic heart failure, including a significant decrease in the mortality rate,<sup>16</sup> have been ascribed to a possible antifibrogenic effect.

This, as well as other observations,<sup>17,18</sup> together with the lack of an evident direct profibrogenic action of aldosterone, have led to the hypothesis that antialdosteronic drugs may exert a direct antifibrogenic action, i.e., independent of their aldosterone antagonism. In addition, attempts to verify this possibility in animal models of liver fibrosis have led to controversial findings.<sup>19-21</sup>

The aim of this study was to evaluate the possible direct antifibrotic effects of canrenone, the active metabolite of spironolactone, in activated human HSC. This potential activity was evaluated by the well-established mitogenic and chemotactic effects exerted by platelet-derived growth factor (PDGF)<sup>22,23</sup> and the increased de novo synthesis of different extracellular matrix (ECM) components induced by transforming growth factor- $\beta$ 1 (TGF- $\beta$ 1).<sup>24,25</sup>

## Materials and Methods

### Reagents

Monoclonal, agarose-conjugated antiphosphotyrosine antibodies were purchased from Oncogene Science (Uniondale, NY). Monoclonal antiphosphotyrosine antibodies for Western blotting were purchased from UBI (Lake Placid, NY). Polyclonal anti-human PDGF type B receptor was purchased from Upstate Biotechnology (Lake Placid, NY). Polyclonal antibodies against extracellular signal-regulated kinase (ERK)-1, phospholipase C- $\gamma$ 1 (PLC- $\gamma$ ), and pp125FAK were purchased from Santa Cruz Biotechnology (Santa Cruz, CA). Myelin basic protein was purchased from Sigma Chemical Co. (St. Louis, MO). Protein A-sepharose was from Pharmacia (Uppsala, Sweden). [ $\gamma$ -<sup>32</sup>P]Adenosine triphosphate (ATP) (3000 Ci/mmol)

and [ $\alpha$ -<sup>32</sup>P]deoxycytidine triphosphate (3000 Ci/mmol) were from New England Nuclear (Milan, Italy). Methyl-[<sup>3</sup>H]thymidine ([<sup>3</sup>H]TdR) was from New England Nuclear. Human recombinant PDGF-BB was purchased from Peprotech (Rock Hill, NJ), and human thrombin was purchased from Boehringer Mannheim GmbH (Mannheim, Germany). Canrenone was provided by GN Pharma (Milan, Italy). Ethylisopropylamiloride (EIPA) was purchased from Sigma Aldrich SRL (Milan, Italy). Cariporide (HOE 642) was kindly provided by Aventis Pharma (Frankfurt a.M., Germany). All other reagents were of analytic grade.

### Isolation and Culture of Human Hepatic Stellate Cells

Human HSC were isolated from wedge sections of normal human liver unsuitable for transplantation, as previously reported.<sup>24,26</sup> Briefly, after digestion with collagenase/pronase, HSC were separated from other liver nonparenchymal cells by ultracentrifugation over gradients of Stractan (Cellsep isotonic solution; Larex Inc., St. Paul, MN). Characterization was performed as described elsewhere.<sup>24</sup> Cells were cultured on plastic culture dishes in Iscove's modified Dulbecco's medium supplemented with 0.6 U/mL of insulin, 2.0 mmol/L of glutamine, 0.1 mmol/L of nonessential amino acids, 1.0 mmol/L of sodium pyruvate, antibiotic-antimycotic solution (all provided by Gibco Laboratories, Grand Island, NY), and 20% fetal bovine serum (Imperial Laboratories, Andover, UK). Experiments described in this study were performed on cells between the first and third serial passages (1:3 split ratio) with 3 independent cell lines. At these stages of culture, human HSC showed transmission electron microscopy features of myofibroblast-like cells, thus indicating complete transition to their activated phenotype.<sup>24</sup>

### DNA Synthesis

DNA synthesis was measured as the amount of [<sup>3</sup>H]TdR incorporated into trichloroacetic acid-precipitable material, as described elsewhere.<sup>22</sup> Briefly, 90% confluent cells were incubated in serum-free/insulin-free (SFIF) medium for 48 hours and stimulated for 20 hours with PDGF-BB (10 ng/mL) in the presence or absence of canrenone, EIPA, or HOE 642. After 4 hours of pulsing with 1.0  $\mu$ Ci/mL of [<sup>3</sup>H]TdR, cells were washed and lysed, and the amount of [<sup>3</sup>H]TdR incorporated was measured. Results were expressed as counts per minute per  $10^5$  cells.

### Cell Growth Assay

A total of  $10^4$  HSC were plated in 12-well dishes and incubated in SFIF for 24 hours. Cells were then stimulated with PDGF-BB (10 ng/mL) in the presence or absence of canrenone (10–50  $\mu$ mol/L) (time 0) for different time periods and counted. Cell counts were performed on triplicate wells on day 0 and after 2, 4, and 6 days. Fresh medium and agonists were added to the remaining wells at each time point.

### Chemotactic Assay

Cell migration was performed as previously described.<sup>23</sup> Briefly, modified Boyden chambers equipped with 8- $\mu\text{m}$ -porosity polyvinylpyrrolidone-free polycarbonate filters were used after precoating (20  $\mu\text{g}/\text{mL}$  of human type I collagen; 30 minutes at 37°C). Confluent HSC were incubated in SFIF medium for 48 hours and then treated with the agonist to be tested. After trypsinization,  $4 \times 10^4$  cells were added to the top chamber and incubated at 37°C for 6 hours. The lower chamber was filled with SFIF medium (control) or PDGF-BB (10 ng/mL) in the presence or absence of the agonist used in the preincubation period. Filters were fixed with 96% methanol and stained with Harris' hematoxylin, mounted, and viewed at 450 $\times$  magnification. Migrated cells were quantified as the mean  $\pm$  SD in 10 randomly chosen high-power fields.

### Wound-Healing Assay

For the measurement of cell migration during wound healing, human HSC were seeded on 6-well plates coated with type I collagen (20  $\mu\text{g}/\text{mL}$ ) and grown to confluence in Iscove's medium containing 20% fetal bovine serum. Confluent cell cultures were incubated in SFIF medium for 48 hours before the beginning of the experiment. Monolayers were then disrupted to generate a linear wound of approximately 1 mm with a cell scraper, washed to remove debris, and incubated in medium containing PDGF-BB (10 ng/mL) in the presence or absence of increasing doses of canrenone for 20 hours. Cells were subsequently fixed and observed by phase contrast microscopy. For the evaluation of wound closure in the different experimental conditions, 5 randomly selected points along each wound were marked, and the horizontal distance of migrating cells from the initial wound was measured at 20 hours after wounding. Experiments were performed in duplicate, and 2 fields of each well were recorded.

### Analysis of Cytotoxicity

Confluent HSC were incubated in SFIF medium for 24 hours and exposed to increasing concentrations of canrenone. Cell viability was evaluated by the trypan blue dye exclusion test at the end of a 24- to 48-hour incubation period.

### Extracellular Signal-Regulated Kinase Assay

ERK was measured as the myelin basic protein kinase activity of ERK immunoprecipitates. Cells were lysed in buffer containing 50 mmol/L of HEPES (pH 7.5), 150 mmol/L of NaCl, 1.0 mmol/L of ethylene glycol-bis( $\beta$ -aminoethyl ether)- $N,N,N',N'$ -tetraacetic acid (EGTA), 1% Triton X-100, 10% glycerol, 1.5 mmol/L of  $\text{MgCl}_2$ , 2 mmol/L of  $\text{Na}_3\text{VO}_4$ , and protease inhibitors. ERKs were immunoprecipitated with anti-ERK2 and subjected to *in vitro* kinase assay. Samples were incubated with 40  $\mu\text{L}$  of kinase buffer (20 mmol/L of HEPES [pH 7.5], 10 mmol/L of  $\text{MgCl}_2$ , 20  $\mu\text{mol}/\text{L}$  of ATP, and 0.5 mmol/L of  $\text{Na}_3\text{VO}_4$ ) containing 5  $\mu\text{Ci}$  of [ $\gamma^{32}\text{P}$ ]ATP and 0.5 mg/mL of myelin basic protein for 30 minutes at room temperature and then separated by sodium dodecyl sulfate-

polyacrylamide gel electrophoresis (SDS-PAGE) (15%). The gels were stained, dried, and exposed to X-Omat AR film (Eastman Kodak, Rochester, NY).

### Northern Blot Analysis

RNA was isolated as previously described.<sup>24</sup> A total of 10  $\mu\text{g}$  of total RNA was fractionated by 1% agarose-formaldehyde gel electrophoresis and blotted on a nylon membrane. Procedures for DNA radiolabeling and filter hybridization were performed as described elsewhere.<sup>27</sup>

### Immunoprecipitation and Immunoblotting

Cells were lysed in 50 mmol/L of HEPES (pH 7.5), 150 mmol/L of NaCl, 1.0% Triton X-100, 5.0 mmol/L of  $\text{MgCl}_2$ , 1.0 mmol/L of EGTA, 2.0 mmol/L of  $\text{Na}_3\text{VO}_4$ , 25  $\mu\text{g}/\text{mL}$  of leupeptin, 10  $\mu\text{g}/\text{mL}$  of pepstatin A, and 2.0 mmol/L of phenylmethylsulfonyl fluoride. Immunoprecipitation, SDS-PAGE, and immunoblotting analysis were performed as previously described.<sup>28</sup> Antibodies bound to polyvinylidene difluoride membranes were detected by chemiluminescence with enhanced chemiluminescence (Amersham Life Sciences, Little Chalfont, UK).

### Phosphatidylinositol 3-Kinase Assay

Phosphatidylinositol 3-kinase (PI 3-K) assay was performed as previously described.<sup>28</sup> Briefly, cells were lysed, and proteins were immunoprecipitated by using antiphosphotyrosine antibodies. After washings, the immunobeads were incubated in 50  $\mu\text{L}$  of 20 mmol/L Tris-HCl (pH 7.5), 100 mmol/L of NaCl, 0.5 mmol/L of EGTA, and 0.5  $\mu\text{L}$  of 20 mg/mL phosphatidylinositol for 10 minutes. After 1  $\mu\text{L}$  of 1 mol/L  $\text{MgCl}_2$  and 10  $\mu\text{Ci}$  of [ $\gamma^{32}\text{P}$ ]ATP were added, the incubation was continued for 10 more minutes. The reaction was stopped by adding 150  $\mu\text{L}$  of chloroform/methanol/37% HCl (10:20:0.2). Samples were extracted and dried. Radioactive lipids were separated by thin-layer chromatography by using chloroform/methanol/30% ammonium hydroxide/water (46:41:5:8). After drying, the plates were autoradiographed. The radioactive spots were then scraped and counted in a beta counter.

### Determination of Akt Activity

Akt activity assay was performed as described.<sup>29</sup> Proteins (150  $\mu\text{g}$ ) were immunoprecipitated by using anti-Akt antibodies and protein G agarose. After 3 washings with washing buffer (20 mmol/L of HEPES [pH 7.5], 40 mmol/L of NaCl, 50 mmol/L of NaF, 1 mmol/L of EDTA, 1 mmol/L of EGTA, 0.5% Nonidet P-40 (Sigma), 20 mmol/L of  $\beta$ -glycerophosphate, 0.5 mmol/L of sodium orthovanadate, 1 mmol/L of phenylmethylsulfonyl fluoride, and 10  $\mu\text{g}/\text{mL}$  of leupeptin, pepstatin, and aprotinin), immunobeads were resuspended in kinase buffer (50 mmol/L of HEPES [pH 7.5], 100 mmol/L of NaCl, 10 mmol/L of  $\text{MgCl}_2$ , 10 mmol/L of  $\text{MnCl}_2$ , 10 mmol/L of  $\beta$ -glycerophosphate, 0.5 mmol/L of sodium orthovanadate, 1 mmol/L of phenylmethylsulfonyl fluoride, and 10  $\mu\text{g}/\text{mL}$  of leupeptin, pepstatin and aprotinin) containing 1  $\mu\text{mol}/\text{L}$  of protein kinase A inhibitor peptide, 50  $\mu\text{mol}/\text{L}$  of unlabeled ATP, and 6  $\mu\text{Ci}$  of [ $\gamma^{32}\text{P}$ ]ATP, with exogenous histone H2B

(1.5  $\mu\text{g}$  per tube) as a substrate, and incubated for 20 minutes at room temperature. Samples were resolved in 12% SDS-PAGE, and gel was subjected to autoradiography.

### Intracellular Calcium Concentration

Digital video imaging of the intracellular free calcium concentration ( $[\text{Ca}^{2+}]_i$ ) in individual human HSC was performed as described.<sup>30</sup> Subconfluent HSC were grown in complete medium on glass coverslips and then incubated for 48 hours in SFIF medium. Cells were then loaded with 4  $\mu\text{mol/L}$  of Fura-2-AM (Calbiochem Corp., San Diego, CA) and 15% Pluronic F-127 (Sigma) for 30 minutes at 22°C.  $[\text{Ca}^{2+}]_i$  was measured in Fura-2-loaded cells in HEPES/ $\text{NaHCO}_3$  buffer containing 140 mmol/L of NaCl, 3 mmol/L of KCl, 0.5 mmol/L of  $\text{NaH}_2\text{PO}_4$ , 12 mmol/L of  $\text{NaHCO}_3$ , 1.2 mmol/L of  $\text{MgCl}_2$ , 1.0 mmol/L of  $\text{CaCl}_2$ , 10 mmol/L of HEPES, and 10 mmol/L of glucose (pH 7.4). Ratio images (340–380 nm) were collected every 3 seconds, and calibration curves were obtained for each cell preparation as described.<sup>26</sup> Stimuli were added directly to the perfusion chamber after the  $[\text{Ca}^{2+}]_i$  basal value was recorded. Cells were preincubated with the drug to be tested 15 minutes before stimulation with PDGF or thrombin. In experiments evaluating changes in the cell area induced by thrombin, spatial calibration was performed by measuring the division on a graticule under the same optical conditions as the rest of the experiments, as reported.<sup>26</sup>

### Measurement of $\text{Na}^+/\text{H}^+$ Antiporter Activity

Human HSC were grown on glass coverslips until 70% confluence and were maintained for 48 hours in SFIF. HSC were loaded with 2  $\mu\text{mol/L}$  of bis-carboxyethylcarboxyfluorescein (BCECF) for 30 minutes at room temperature and then washed. Fluorescence was recorded in individual cells by using an imaging analysis system equipped for epifluorescence. Ratio imaging was obtained every 3 seconds, alternating excitation wavelengths at 490 nm and 405 nm, with emission at 520 nm. In experiments aimed at evaluating the effect of canrenone on the basal activity of the  $\text{Na}^+/\text{H}^+$  antiporter, HSC were acidified by adding 5  $\mu\text{mol/L}$  of nigericin in nominally  $\text{Na}^+/\text{K}^+$ -free *N*-methylglucamine buffer. In this setting, a decrease in the fluorescence ratio indicates a decrease in cytosolic pH. When the fluorescence ratio value had stabilized, the administration of 30 mmol/L of NaCl caused a rapid cytosolic alkalization, indicating restored  $\text{Na}^+/\text{H}^+$  antiporter activity; the kinetic of alkalization is an index of the  $\text{Na}^+/\text{H}^+$  antiporter activity. EIPA and HOE 642, both regarded as specific  $\text{Na}^+/\text{H}^+$  antiporter inhibitors, were used as control drugs. In experiments evaluating the effect of canrenone, as well as other drugs, on PDGF-induced changes in intracellular pH concentration ( $[\text{pH}]_i$ ), cells were preincubated with the drug to be tested 15 minutes before the stimulation with PDGF.

### Metabolic Labeling and Immunoprecipitation

Metabolic labeling and immunoprecipitation were performed as described previously.<sup>14,31</sup> Briefly, subconfluent cultures were incubated 24 hours with SFIF medium before treatment with canrenone, TGF- $\beta$ 1, or both. One group of

HSC was treated with 25  $\mu\text{mol/L}$  of canrenone, and another group was exposed to 1 ng/mL of TGF- $\beta$ 1. The third group was treated with canrenone for 1 hour, followed by an incubation with TGF- $\beta$ 1 for 24 hours. De novo protein synthesis of exposed HSC was compared with that of nontreated cells. After the initial 24 hours of treatment, cells were cultured in methionine-free Dulbecco's modified Eagle medium and were metabolically labeled for 24 hours with 50  $\mu\text{Ci/mL}$  of  $^{35}\text{S}$ -methionine/cysteine (trans  $^{35}\text{S}$ -label; specific activity, >1000 Ci/mmol; ICN Biomedicals, Costa Mesa, CA) in the presence of vitamin C (50  $\mu\text{g/mL}$ ) (Merck, Darmstadt, Germany) and  $\beta$ -aminopropionitrile (64  $\mu\text{g/mL}$ ) (Sigma) while exposure to canrenone, TGF- $\beta$ 1, or both was continued. Labeled media and cell layers were separately harvested and stored at  $-70^\circ\text{C}$ . Total protein synthesis was assessed by trichloroacetic acid precipitation. The labeled media or cell lysates were subjected to immunoprecipitation with specific antibodies against collagen type I (Southern Biotechnology, Birmingham, AL), smooth muscle  $\alpha$ -actin (clone 1A4; Sigma), or the N-terminal propeptide of procollagen type III.<sup>32</sup> For collagen type I and IV, incubation with the primary antibody was followed by incubation with affinity-purified rabbit anti-goat immunoglobulin G (Jackson Immunochemicals, West Grove, PA) as a second antibody for 1 hour at  $4^\circ\text{C}$ .<sup>14,31</sup> After immunoprecipitation, proteins were separated by SDS-PAGE, followed by enhancement with Amplify (Amersham), dried, and exposed to preflashed Hyperfilm-MP (Amersham). Band intensities were quantified by Phosphor Imaging (Molecular Imager, GS-525; Bio-Rad, Hercules, CA). The ratio of [ $^{35}\text{S}$ ]methionine/[ $^{35}\text{S}$ ]cysteine incorporation into the protein of treated cells over control cells—hereafter referred to as the treated/control ratio—was calculated for each condition and expressed as mean  $\pm$  SD. At least 3 independent observations (cells of 3 different cultures) were used to calculate the mean. The results are presented as bar graphs, with the control values normalized at 100. Immunoprecipitation was performed on an aliquot of cell layer and medium containing  $5.0 \times 10^5$  or  $1.0 \times 10^6$  cpm. This aliquot was a known fraction of the radioactivity in the cell layer and medium. To determine the statistical significance of the difference between control and treated cells, 95% confidence intervals were calculated. The effect was considered statistically significant when 100 (normalized control value) did not belong to the 95% confidence interval of the treated/control ratio.

### Measurement of Aldosterone Levels in Activated Human Hepatic Stellate Cell Supernatants

Conditioned medium was obtained from different preparations of activated human HSC. Cells were grown to confluence in 100-mm Petri dishes in complete culture medium. After extensive washing with SFIF medium, confluent cells were incubated for 24 hours in SFIF. Supernatants were then harvested, and aliquots from each batch were concentrated 2 $\times$  and 4 $\times$ . Aldosterone levels were measured by radioimmunoassay with the Aldosterone/RIA-KS17CT kit (Radim, S.p.A., Pomezia, Italy). The lower detection limit for this assay is 0.007 nmol/L.

## Statistical Analysis

Unless otherwise specified, results, relative to the number of experiments indicated, are expressed as means  $\pm$  SD. Statistical analysis was performed by 1-way analysis of variance and, when the *F* value was significant, by Duncan's test.

## Results

### Canrenone Reduces PDGF-Induced Cell Proliferation and Migration

The effect of increasing concentrations of canrenone on PDGF-BB-induced DNA synthesis, measured as [ $^3\text{H}$ ]thymidine incorporation into DNA, was evaluated first. As shown in Figure 1A, preincubation with canrenone for 5 minutes induced a dose-dependent inhibition of PDGF-induced mitogenesis. This inhibitory effect was statistically significant starting at 5  $\mu\text{mol/L}$ . Growth curves for activated human HSC in response to PDGF-BB with or without canrenone were analyzed to determine whether the decrease in PDGF-induced DNA synthesis was associated with an actual decrease in cell growth. As illustrated in Figure 1B, PDGF-BB at the dose of 10 ng/mL significantly increased HSC growth after 2 and 4 days of incubation when compared with unstimulated control cells. This effect was clearly reduced by pretreatment with canrenone, and this reduction was already statistically significant after 2 days of culture.

When cells were treated with canrenone alone, a decrease in [ $^3\text{H}$ ]thymidine incorporation was observed at 50  $\mu\text{mol/L}$  or higher concentrations (Figure 1A). To exclude toxic effects of canrenone in these experimental conditions, different concentrations of canrenone were tested for cytotoxicity on cells maintained for 24 or 48 hours in SFIF medium. No significant toxic effect was detected at any concentration tested.

To evaluate the effect of canrenone on cell motility, 2 different experimental approaches were used: the evaluation of chemotaxis in a modified Boyden chamber system and the wound-healing migration assay. As illustrated in Figure 2A, incubation of HSC with PDGF-BB for 6 hours stimulated cell haptotaxis. In the presence of canrenone, this effect was reduced dose-dependently. Figure 2B shows wounded monolayers incubated in medium containing PDGF-BB without or with increasing doses of canrenone. PDGF induced cell migration leading to wound closure 20 hours after wounding. In the presence of canrenone, PDGF-induced cell migration in the wounded area was inhibited in a dose-dependent fashion. The percentage of inhibition, measured on the whole wound length, was 37%, 56%, 74%, and 90% in response to 5, 10, 25, and 50  $\mu\text{mol/L}$  of canrenone, respectively.

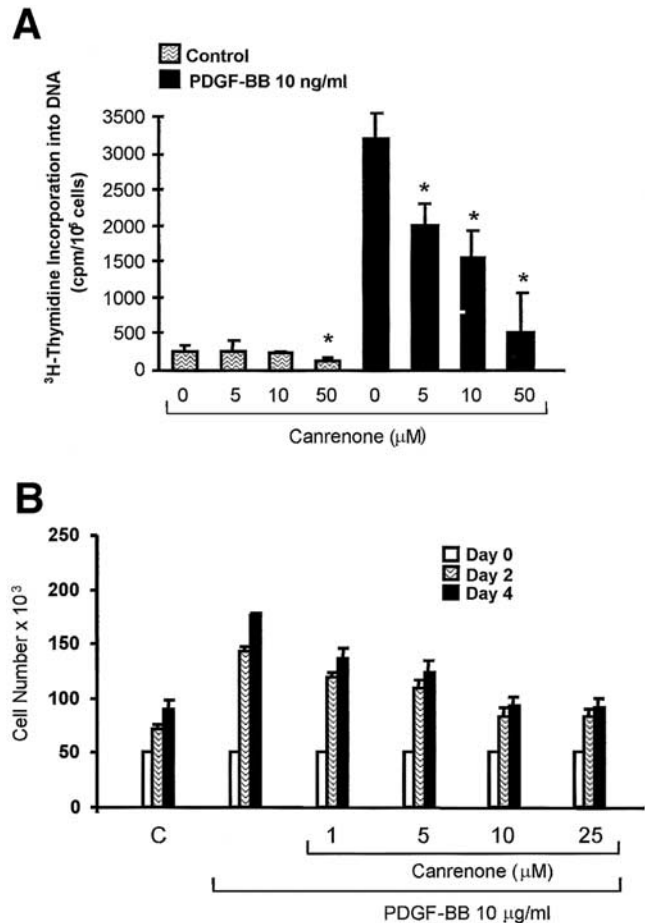


**Figure 1.** Effect of canrenone on cell proliferation in activated human HSC. (A) Dose response for the effect of increasing concentrations of canrenone on PDGF-induced DNA synthesis, evaluated as [ $^3\text{H}$ ]TdT incorporation into DNA. Confluent cells were incubated for 48 hours in SFIF medium and then pretreated for 5 minutes with increasing concentrations of canrenone before starting an incubation with PDGF-BB (10 ng/mL) for 24 hours. Cells were pulsed with [ $^3\text{H}$ ]TdT during the last 4 hours of incubation. Data are mean  $\pm$  SD for 3 experiments performed in triplicate. Compared with the effect of PDGF alone, changes were statistically significant ( $*P < 0.05$  or higher degree of significance) starting at 5  $\mu\text{mol/L}$  of canrenone. (B) Effect of canrenone on cell proliferation. HSC were plated on 12-well dishes at a density of  $6 \times 10^4$  in complete culture medium. After 24 hours (day 0), cells were washed with SFIF medium and incubated in fresh SFIF alone (control) or PDGF-BB (10 ng/mL) with or without increasing doses of canrenone. At each time point, cells were trypsinized and counted with a Coulter cell counter. Fresh medium containing the same test conditions was added to the remaining wells at day 2. Data are the mean values  $\pm$  SD for 2 experiments performed in quadruplicate. Changes were statistically significant starting at day 4 for all doses of canrenone tested. C, control, not treated.

### Effect of Canrenone on Platelet-Derived Growth Factor-Induced Intracellular Signaling

To investigate the mechanisms responsible for the effect of canrenone on PDGF-induced cell proliferation and migration, we first analyzed the effects of

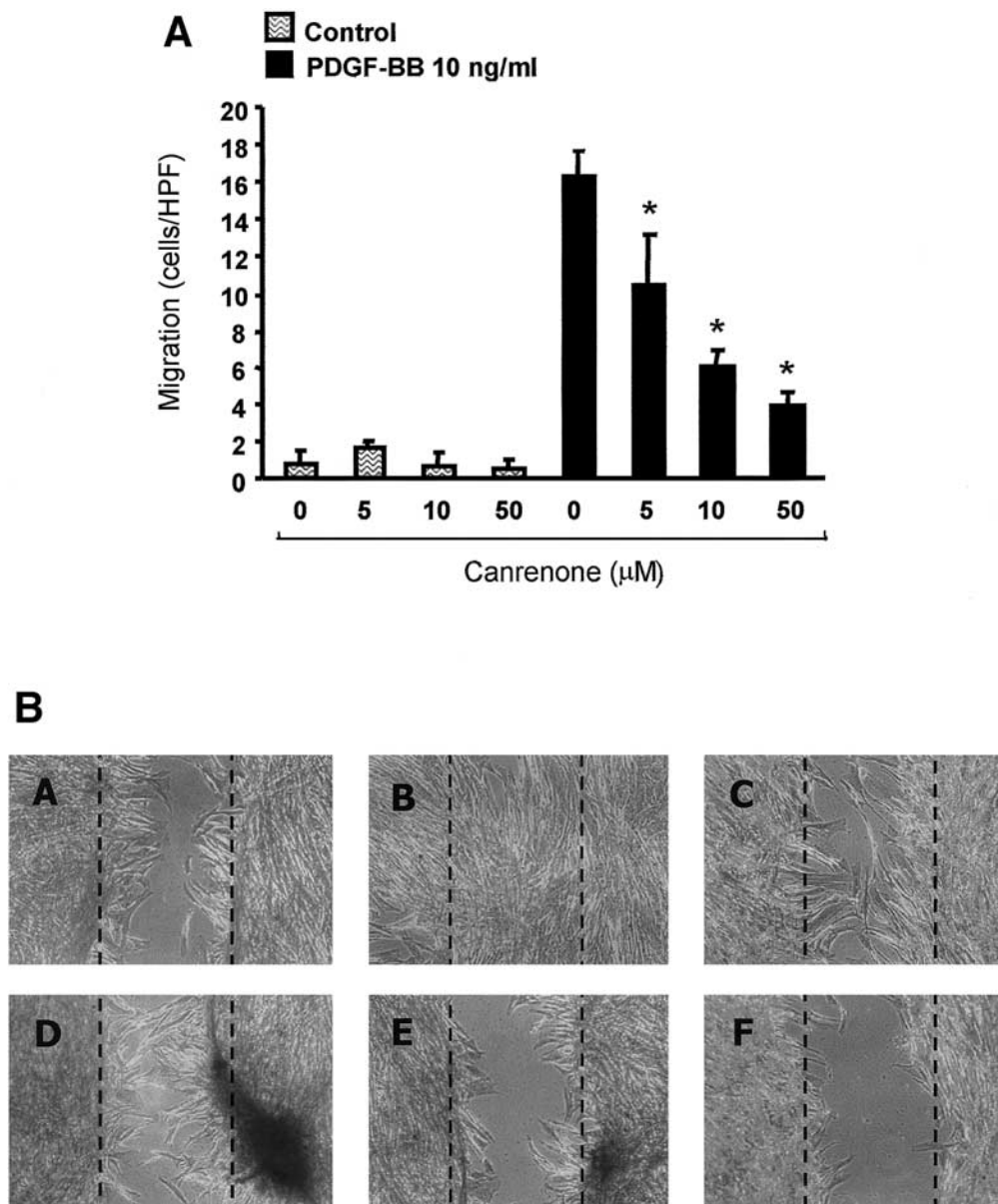


**Figure 2.** Effect of canrenone on PDGF-induced chemotaxis in activated human HSC. (A) Cell migration was determined in modified Boyden chambers as described in Materials and Methods;  $4 \times 10^4$  cells were seeded in SFIF medium in the upper compartment of the Boyden chamber and were tested for migration in the lower chamber through a filter precoated with collagen type I. Cells that migrated to the lower surface of the filter after 6 hours were stained and quantified by cell counting. Values (cells migrated per high-power field [HPF]) are expressed as mean  $\pm$  SD and are from 8 separate fields counted from 3 different experiments. Compared with the effect of PDGF alone, changes were statistically significant ( $*P < 0.05$  or higher degree of significance) starting at 5  $\mu\text{mol/L}$  of canrenone. (B) Wound-healing assay. Human HSC were seeded on 6-well plates coated with type I collagen (20  $\mu\text{g/mL}$ ) and grown to confluence in Iscove's medium containing 20% fetal bovine serum. Confluent cell cultures were incubated in serum-free/insulin-free (SFIF) medium for 48 hours before the beginning of the experiment. Monolayers were then disrupted to generate a linear wound with a cell scraper of approximately 1 mm, washed to remove debris, and incubated in medium containing PDGF-BB (10 ng/mL) in the presence or absence of increasing doses of canrenone for 20 hours (A, control; B, PDGF; C, PDGF plus canrenone 5  $\mu\text{mol/L}$ ; D, PDGF plus canrenone 10  $\mu\text{mol/L}$ ; E, PDGF plus canrenone 25  $\mu\text{mol/L}$ ; and F, PDGF plus canrenone 50  $\mu\text{mol/L}$ ). Monolayers were then fixed and photographed by phase contrast microscopy. For the evaluation of wound closure in the different experimental conditions, 5 randomly selected points along each wound were marked, and the horizontal distance of migrating cells from the initial wound was measured at 20 hours after wounding. Experiments were performed in duplicate, and 2 fields of each well were recorded.

canrenone on PDGF- $\beta$  receptor phosphorylation and the resulting activation of downstream pathways, such as PLC- $\gamma$ , ERK, and PI 3-K. HSC were pretreated for 5 minutes with increasing concentrations of canrenone

and then exposed to PDGF-BB (10 ng/mL) for 10 minutes. As shown in Figure 3A, in the absence of canrenone, PDGF induced a marked increase in PDGF- $\beta$  receptor tyrosine phosphorylation. Can-

renone, at any concentration used, had no effect on this signaling event. Similarly, canrenone did not affect PDGF-induced PLC- $\gamma$  phosphorylation (Figure 3B), PDGF-induced ERK activity (Figure 3C), or *c-fos* gene expression, a nuclear target of ERK activation (Figure 3D).

In contrast, canrenone inhibited PDGF-induced PI 3-K activity. As shown in Figure 4A, exposure of serum-deprived HSC to PDGF-BB for 10 minutes resulted in the activation of PI 3-K. Incubation with canrenone 5 minutes before the addition of PDGF-BB dose-dependently inhibited PI 3-K activity. To establish whether the action of canrenone on PI 3-K

occurred directly, extracts obtained from PDGF-treated HSC were immunoprecipitated with anti-phosphotyrosine antibodies and then exposed in vitro to increasing doses of canrenone before the kinase assay was performed (Figure 4B). Also, in these conditions, an inhibitory effect was observed, indicating a direct inhibition of canrenone on this enzymatic activity. To confirm these findings, we also tested the effects of canrenone on the activation of Akt, which lies downstream of PI 3-K. In agreement with the data on PI 3-K, canrenone significantly reduced the phosphorylation of Akt induced by PDGF (Figure 5).

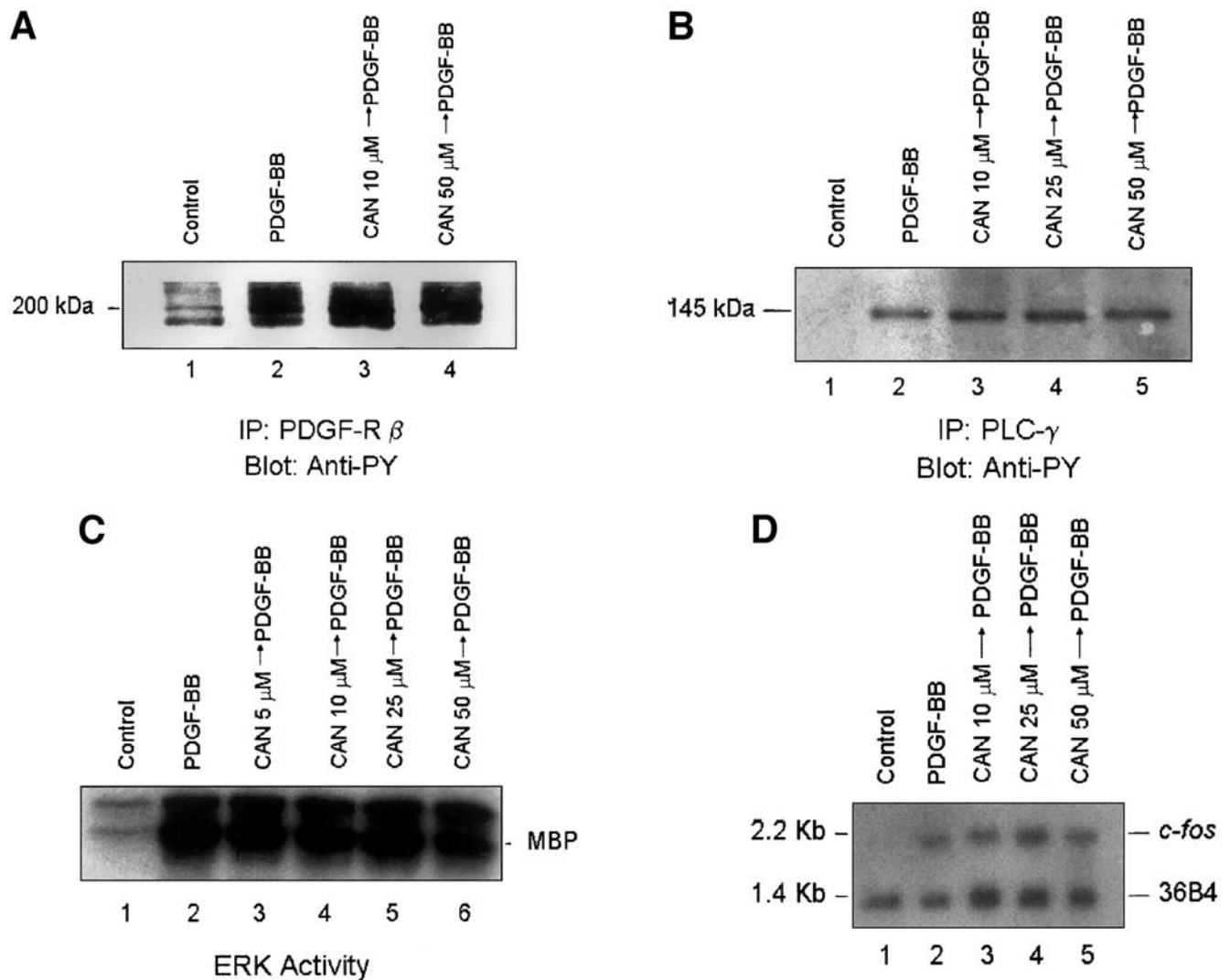


**Figure 3.** Effect of canrenone (CAN) on PDGF signaling pathways. Confluent HSC were incubated for 48 hours in SFIF medium and then treated with different doses of canrenone 5 minutes before stimulation with PDGF-BB (10 ng/mL) for 10 minutes. (A and B) Western blot analysis; 100  $\mu$ g of proteins were immunoprecipitated with antibodies against PDGF-R  $\beta$  (A) or PLC- $\gamma$  (B). The immunoprecipitates (IP) were analyzed by 7.5% SDS-PAGE, followed by immunoblotting with antiphosphotyrosine (PY). (C) ERK assay. Cell lysates were immunoprecipitated with anti-ERK2 antibody and subjected to an immune complex kinase assay with myelin basic protein (MBP) as a substrate. (D) Expression of *c-fos* messenger RNA; 10  $\mu$ g of total RNA extracted from treated or untreated (control) HSC was analyzed by Northern blot. The *c-fos* complementary DNA probe was then removed by boiling, and the same blot was hybridized to a complementary DNA encoding for the ribosomal protein 36B4 (control gene).



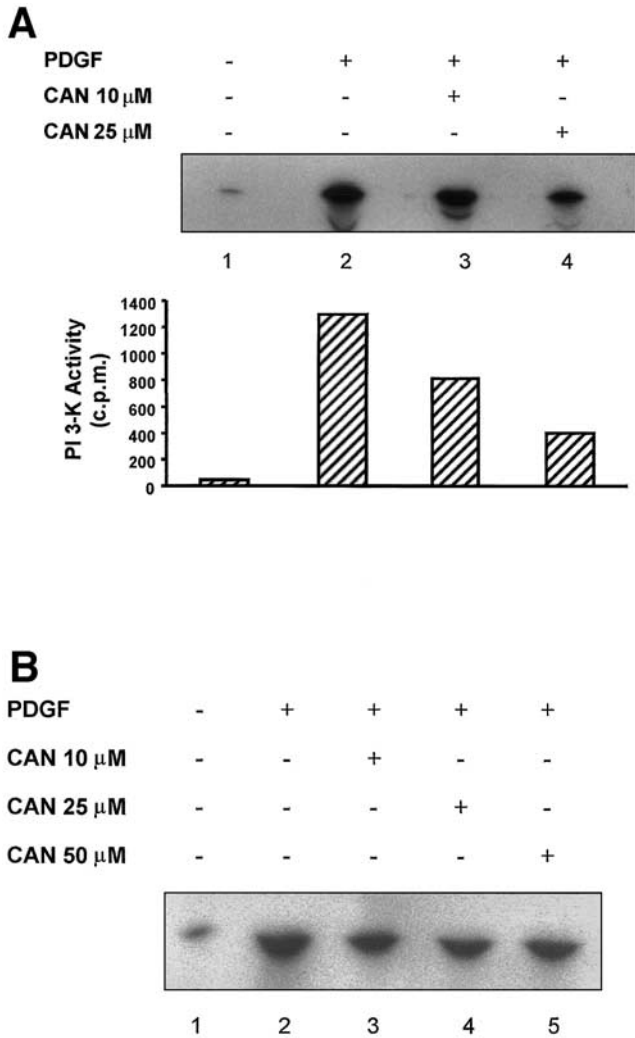


**Figure 4.** Canrenone (CAN) dose-dependently inhibits PI 3-K activation induced by PDGF in human HSC. (A) Confluent cells were maintained in SFIF medium for 48 hours and then pretreated with canrenone (10 or 25  $\mu$ mol/L) 5 minutes before stimulation with PDGF (10 ng/mL) for 10 minutes. Equal amounts of proteins were immunoprecipitated with antiphosphotyrosine antibody, and immunobeads were assayed for PI 3-K activity as described in Materials and Methods. A representative experiment of 3 is shown. (B) Cell lysates extracted from either untreated (control) or PDGF-stimulated HSC were immunoprecipitated with anti-phosphotyrosine antibodies. After washings, samples shown in lanes 3, 4, and 5 were incubated in vitro with increasing doses of canrenone for 10 minutes. The kinase assay was performed as previously described. A representative experiment of 2 is shown.

### Effect of Canrenone on Intracellular pH and $Ca^{2+}$ Concentration

Because it has been shown that PDGF signaling involves changes in  $[Ca^{2+}]_i$  and  $[pH]_i$  in HSC, we next investigated whether canrenone could modulate these effects.<sup>30,33,34</sup> We first evaluated the effect of this drug on the basal activity of the  $Na^+/H^+$  exchanger (NHE) that regulates  $[pH]_i$  in HSC. As illustrated in Figure 6, untreated cells (control) recovered readily from an

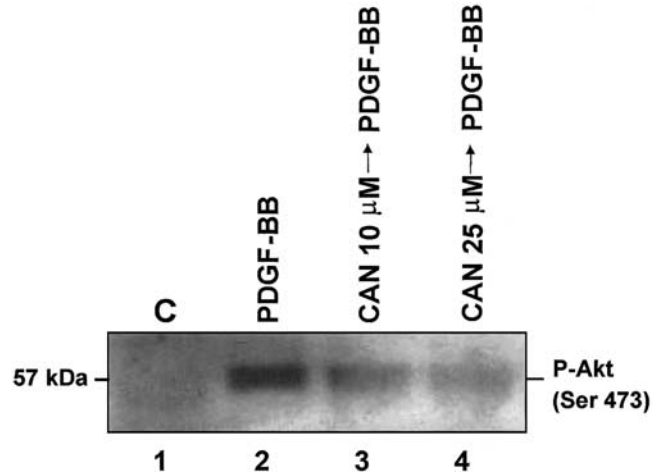


**Figure 5.** Canrenone (CAN) reduces PDGF-induced Akt activity. Starved HSC were pretreated with canrenone (10 or 50  $\mu$ mol/L) 5 minutes before stimulation with PDGF (10 ng/mL) for 10 minutes. Cell lysates were immunoprecipitated with anti-Akt antibodies, and an immune complex kinase assay was performed by using histone H2B as a substrate. C, control, not treated. A representative experiment of 3 is shown.

acute acid load in a  $Na^+$ -free medium on reintroduction of  $Na^+$ . Treatment with canrenone, in a dose range between 10 and 25  $\mu$ mol/L, did not significantly affect the antiporter activity. However, when canrenone was used at the dose of 50  $\mu$ mol/L, the

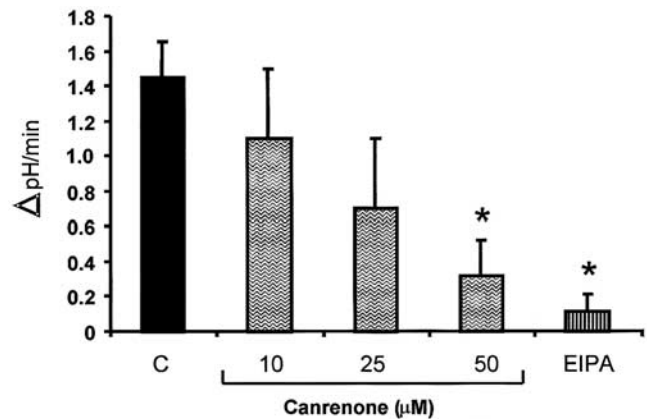


**Figure 6.** Effect of canrenone on basal  $Na^+/H^+$  exchanger activity (pH recovery after nigericin-induced acid load). Human HSC were grown on coverslips until 70% confluence and incubated in SFIF for 48 hours. Cells were loaded with BCECF, and fluorescence was recorded in individual cells every 3 seconds, alternating excitation wavelengths at 490 nm and 405 nm, at emission 520 nm. HSC were acidified by adding 5  $\mu$ mol/L of nigericin in nominally  $Na^+$ - and  $K^+$ -free *N*-methylglucamine buffer. The administration of 30 mmol/L of NaCl caused a rapid cytosolic alkalinization, indicating restored  $Na^+/H^+$  antiporter activity. Barograms express the kinetic of alkalinization ( $\Delta$  variation of  $[pH]_i$ ) as an index of the  $Na^+/H^+$  antiporter activity and are the mean  $\pm$  SD of 3 experiments, each performed on 20 individual cells. Changes in basal  $Na^+/H^+$  antiporter activity (C) were statistically significant when canrenone was used at 50  $\mu$ mol/L. The  $Na^+/H^+$  antiporter inhibitor EIPA (10  $\mu$ mol/L) was used as positive control. \* $P < 0.05$  or higher degree of significance.

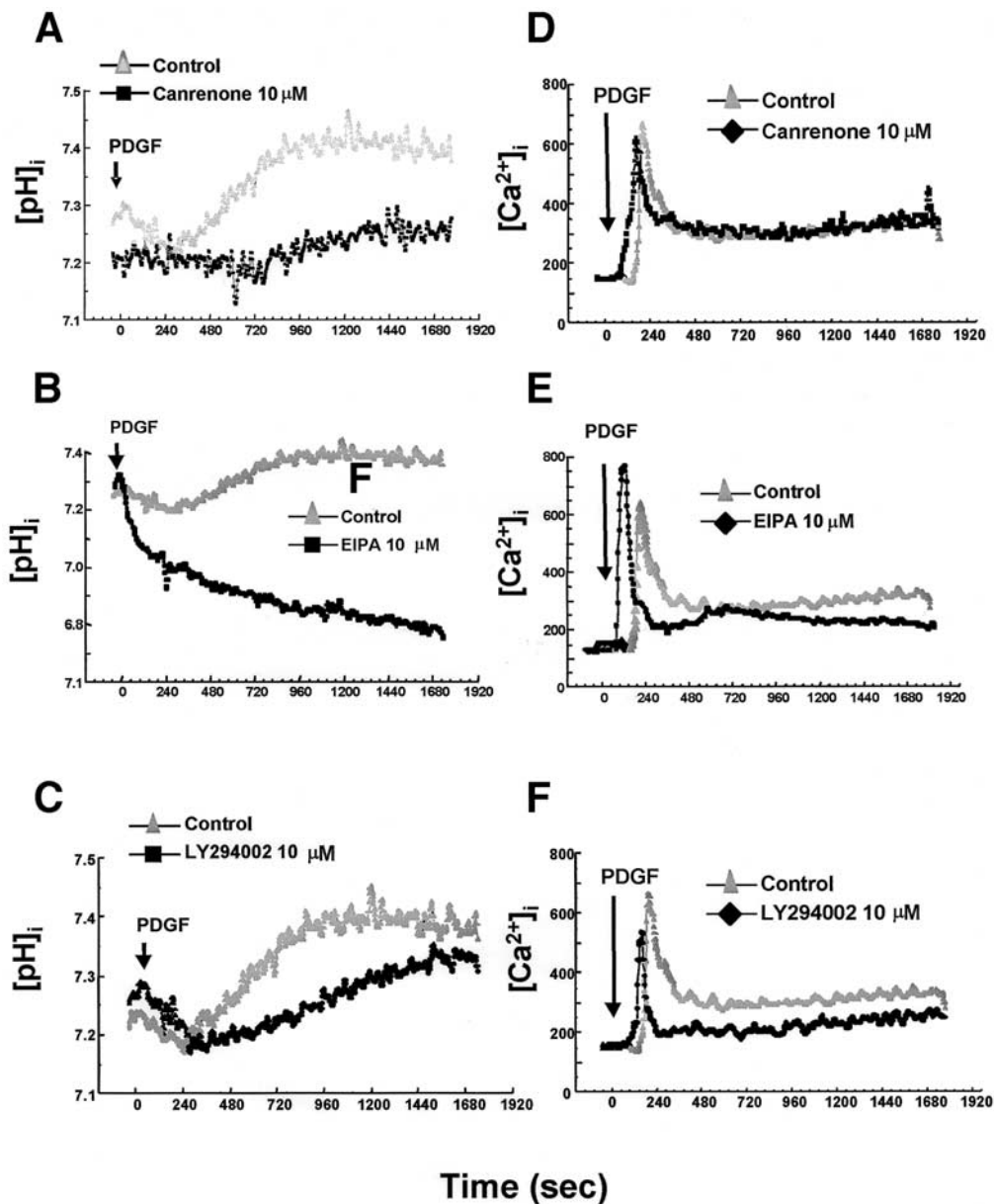


**Figure 7.** Effect of canrenone on PDGF-induced  $\text{Na}^+/\text{H}^+$  antiporter activity and on the PDGF-stimulated increase in  $[\text{Ca}^{2+}]_i$ . Subconfluent (70%–80% confluent) HSC were maintained in SFIF for 48 hours and were then loaded with BCECF to determine  $[\text{pH}]_i$  or with Fura 2-AM to evaluate  $[\text{Ca}^{2+}]_i$ , as described in Materials and Methods. PDGF-BB (10 ng/mL) was added at the arrow (time 0). The tracings illustrate the changes in  $[\text{pH}]_i$  (A, C, and E) or in  $[\text{Ca}^{2+}]_i$  (B, D, and F) induced by PDGF without (control) or with a 10-minute preincubation with canrenone (A and D), EIPA (B and E), or LY294002 (C and F) (all 10  $\mu\text{mol/L}$ ). Data are the mean of 25 determinations in individual cells for each condition used. For each single point, the SD did not exceed 15% of the mean value. Measurements were obtained in individual cells at 3-second time intervals.

activity of the NHE was blocked similarly to the effect of EIPA, an established  $\text{Na}^+/\text{H}^+$  antiporter inhibitor.

In a different set of experiments, we studied the effect of canrenone on PDGF-induced antiporter activity. As shown in Figure 7A, exposure of serum-deprived HSC to PDGF-BB (10 ng/mL) increased  $[\text{pH}]_i$  through the activation of the NHE, and canrenone was able to reduce this increase starting at the concentration of 10  $\mu\text{mol/L}$ . Figure 7B illustrates the inhibitory effect exerted by EIPA, used as positive control. Similar inhibitory effects were produced by the more selective antiporter inhibitor HOE 642 (data not shown). To establish whether PI 3-K was involved in the antiporter activation induced by PDGF, cells were preincubated with LY294002 (Figure

7C) and wortmannin (not shown) before stimulation with PDGF. Both PI 3-K inhibitors reproduced the inhibitory action of canrenone, thus showing the involvement of PI 3-K in PDGF-induced activation of the antiporter. Incubation with PI 3-K inhibitors (LY294002 or wortmannin) in the absence of PDGF did not affect the antiporter activity after an acid load (data not shown).

We next evaluated the effect of these compounds on the changes in  $[\text{Ca}^{2+}]_i$ . As previously shown,<sup>30</sup> treatment with PDGF induced in HSC an increase in  $[\text{Ca}^{2+}]_i$  that was characterized by a peak phase, followed by a long-lasting plateau (Figure 7D). Canrenone did not inhibit either the peak increase or the plateau phase at any of the concentrations tested. No

inhibitory effect was observed when cells were preincubated with antiporter inhibitors (EIPA or HOE 642) or PI 3-K inhibitors (LY294002 or wortmannin) (Figure 7E and F).

#### Effect of Na<sup>+</sup>/H<sup>+</sup> Exchanger Inhibitors on Platelet-Derived Growth Factor-Induced Phosphatidylinositol 3-Kinase Activity and Biological Effects

Because of the observed effect of PI 3-K inhibitors on the activity of the NHE and the possible relationship between PI 3-K activity and this antiporter,<sup>35-37</sup> we next evaluated the effect of EIPA and HOE 642 on PDGF-induced PI 3-K activity. As shown in Figure 8A, pretreatment with 10 μmol/L of EIPA significantly reduced PDGF-induced PI 3-K activity, thus indicating that this established antiporter inhibitor is also a PI 3-K inhibitor. Conversely, the recently introduced and more selective antiporter inhibitor HOE 642 did not show any effect on PDGF-induced PI 3-K activity, even when it was used at the maximal dose of 100 μmol/L (Figure 8B). Because of their different effects on PDGF-induced PI 3-K activity, we investigated whether the antiporter inhibitors EIPA and HOE 642 could reproduce the effects of canrenone on the main biological actions of PDGF in cultured HSC, namely, mitogenesis and chemotaxis. Both compounds inhibited, in a dose-dependent manner, DNA synthesis (Figures 9A and 10A) and cell motility (Figures 9B and 10B) induced by PDGF in activated HSC, thus indicating that Na<sup>+</sup>/H<sup>+</sup> antiporter activity is indispensable for these biological effects of PDGF.

#### Effects of Canrenone and Na<sup>+</sup>/H<sup>+</sup> Antiporter Inhibitors on Platelet-Derived Growth Factor-Induced Focal Adhesion Kinase Phosphorylation

Because the activity of the Na<sup>+</sup>/H<sup>+</sup> antiporter has been shown to be involved in the regulation of integrin-mediated intracellular signaling that leads to cytoskeletal reorganization after stimulation with growth factors,<sup>38,39</sup> we tested whether canrenone, as well as Na<sup>+</sup>/H<sup>+</sup> antiporter inhibitors, could influence PDGF-induced focal adhesion kinase (FAK) phosphorylation in human HSC. FAK is a nonreceptor tyrosine kinase that has been shown to play a central role in integrin-related signaling events. As illustrated in Figure 11, incubation of cells with PDGF-BB (10 ng/mL) for 10 minutes induced an increase in FAK tyrosine phosphorylation, as previously documented.<sup>40,41</sup> Canrenone was able to reduce this increase in a dose-dependent manner. This effect was comparable to that

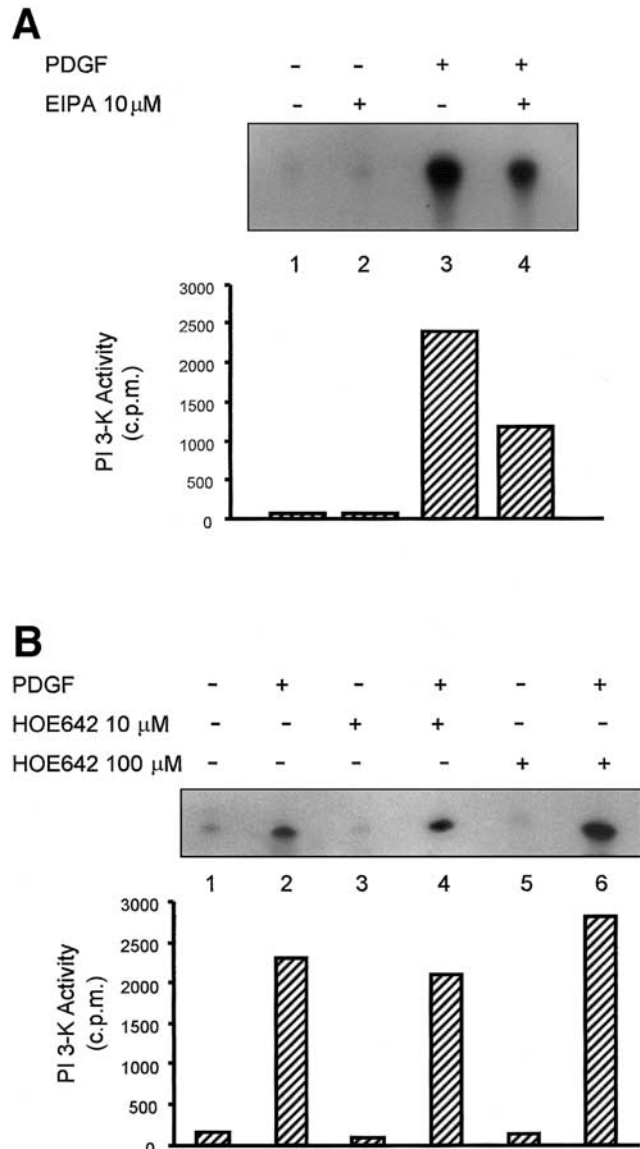


**Figure 8.** Effects of EIPA and HOE 642 on PDGF-induced PI 3-K activity in human HSC. Confluent cells were maintained in SF12 medium for 48 hours and then pretreated with EIPA (10 μmol/L) (A) or HOE 642 (10 and 100 μmol/L) (B) for 5 minutes before stimulation with PDGF-BB (10 ng/mL) for 10 minutes. PI 3-K activity was evaluated as described previously. A representative experiment of 2 is shown.

observed when cells were incubated with EIPA or HOE 642.

#### Effects of Canrenone on the De Novo Synthesis of Different Extracellular Matrix Components

In this set of experiments, additional potential antifibrogenic properties of canrenone were evaluated—particularly the effect of this drug on TGF-β1-induced de novo synthesis of different ECM compo-

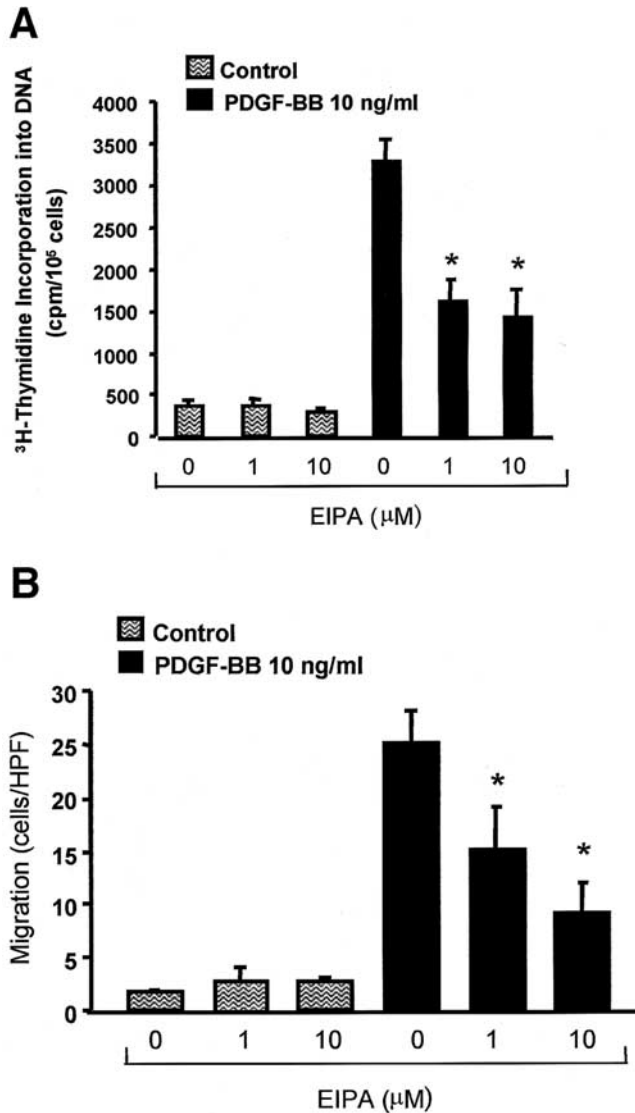


**Figure 9.** Effect of EIPA on PDGF-induced DNA synthesis and chemotaxis in activated human HSC. (A) DNA synthesis was evaluated as the incorporation of [<sup>3</sup>H]TdR into DNA, induced by PDGF, as described in Materials and Methods. Confluent cells were incubated for 48 hours in SFIF medium and then pretreated for 5 minutes with EIPA (5–10 μmol/L) before an incubation was started with PDGF-BB (10 ng/mL) for 24 hours. Cells were pulsed with [<sup>3</sup>H]TdR during the last 4 hours of incubation. Data are mean ± SD for 3 experiments performed in triplicate. Compared with the effect of PDGF alone, changes were statistically significant (\**P* < 0.05 or higher degree of significance) starting at 1 μmol/L of EIPA. (B) Cell motility was measured in modified Boyden chambers as described in Materials and Methods. Values (cells migrated per high-power field [HPF]) are expressed as mean ± SD and are from 8 separate fields counted from 3 different experiments. Compared with the effect of PDGF alone, changes were statistically significant (\**P* < 0.05 or higher degree of significance) starting at 1 μmol/L of EIPA.

nents, namely, procollagen type I, procollagen type IV, and fibronectin. As illustrated in Figure 12, treatment of cell cultures with canrenone (25 μmol/L) did not affect basal synthesis of the different ECM com-

ponents. However, pretreatment with the same dose of canrenone significantly reduced TGF-β1-induced de novo synthesis of procollagen type I and fibronectin, as detected both in cell supernatants and cell monolayers. TGF-β1-induced de novo synthesis of procollagen type IV was significantly reduced only in cell monolayers.

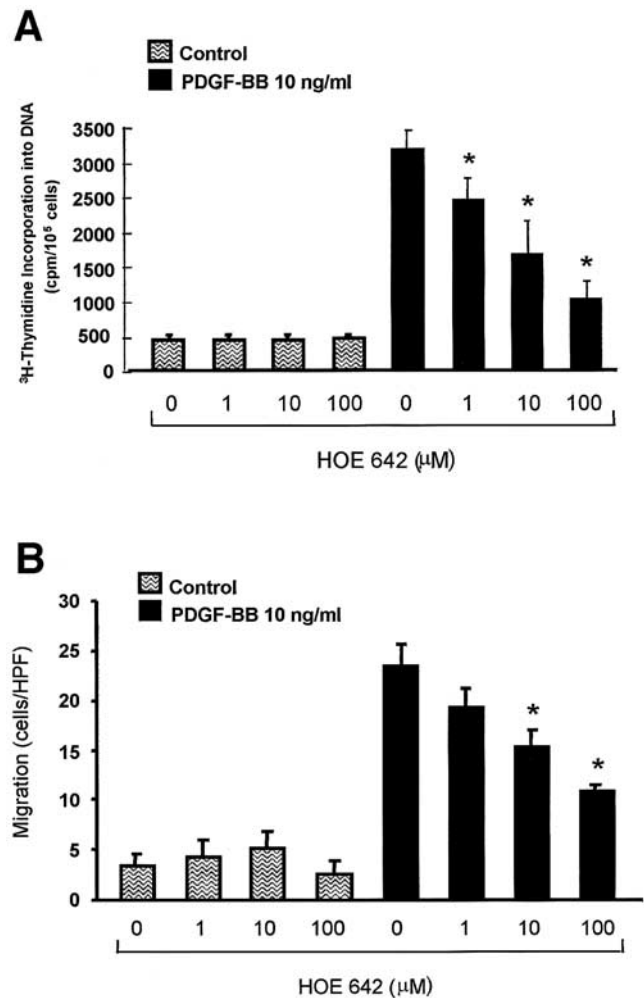
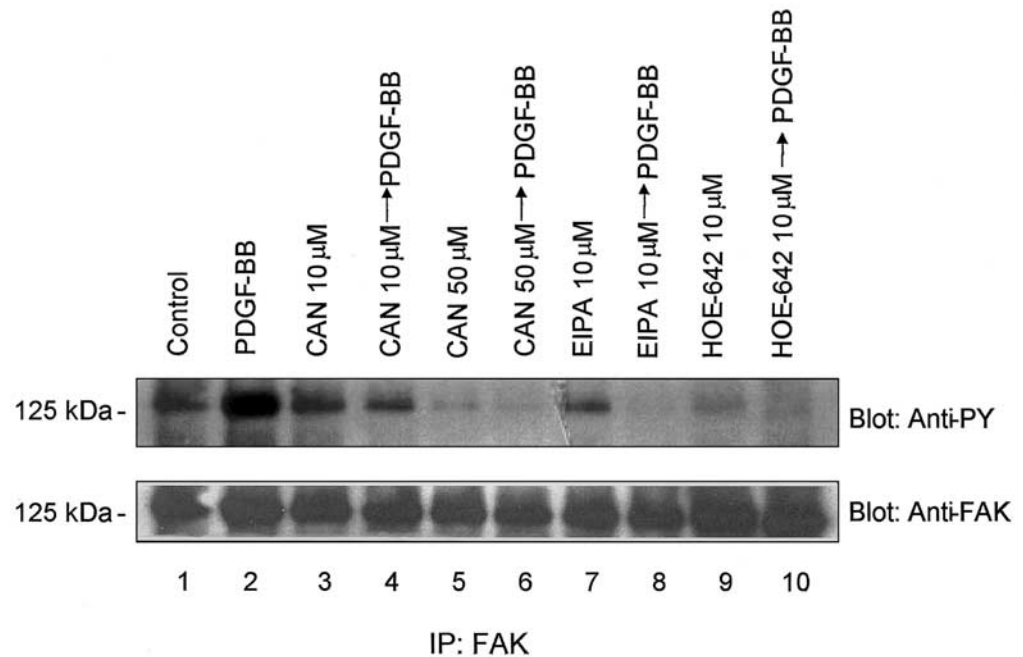


**Figure 10.** Effect of HOE 642 on PDGF-induced DNA synthesis and chemotaxis in activated human HSC. (A) DNA synthesis was evaluated as the incorporation of [<sup>3</sup>H]TdR into DNA, induced by PDGF, as described in Materials and Methods. Confluent cells were incubated for 48 hours in SFIF medium and then pretreated for 5 minutes with HOE 642 (1, 10, and 100 μmol/L) before an incubation was started with PDGF-BB (10 ng/mL) for 24 hours. Cells were pulsed with [<sup>3</sup>H]TdR during the last 4 hours of incubation. Data are mean ± SD for 3 experiments performed in triplicate. Compared with the effect of PDGF alone, changes were statistically significant (\**P* < 0.05 or higher degree of significance) starting at 1 μmol/L of HOE 642. (B) Cell motility was measured in modified Boyden chambers as described in Materials and Methods. Values (cells migrated per high-power field [HPF]) are expressed as mean ± SD and are from 8 separate fields counted from 3 different experiments. Compared with the effect of PDGF alone, changes were statistically significant (\**P* < 0.05 or higher degree of significance) starting at 10 μmol/L of HOE 642.

**Figure 11.** Effect of canrenone (CAN), EIPA, and HOE 642 on PDGF-induced FAK phosphorylation in activated human HSC. Confluent HSC were incubated 48 hours in SFIF medium and then treated with canrenone (10 and 50  $\mu\text{mol/L}$ ), EIPA (10  $\mu\text{mol/L}$ ), and HOE 642 (10  $\mu\text{mol/L}$ ) 5 minutes before stimulation with PDGF-BB (10 ng/mL) for 10 minutes. Equal amounts of protein were immunoprecipitated with an anti-FAK antibody. The immunoprecipitates (IP) were analyzed by 7.5% SDS-PAGE followed by immunoblotting with antiphosphotyrosine (PY) antibody. This antibody was removed, and the membrane was blotted with the same antibody used for immunoprecipitation (anti-FAK). A representative experiment of 3 is shown.



#### Effect of Canrenone on Thrombin-Induced Intracellular Calcium Concentration Increase and Cell Contraction in Activated Human Hepatic Stellate Cells

Because the effects of antialdosteronic drugs on portal pressure have been shown in several clinical and experimental studies,<sup>2-5</sup> we then explored whether canrenone is able to reduce thrombin-induced intracellular calcium increase and cell contraction in activated human HSC. As previously reported,<sup>26</sup> stimulation of human HSC with thrombin resulted in increased  $[\text{Ca}^{2+}]_i$  coupled with a transient reduction of cell area, indicating reversible cell contraction. As shown in Figure 13, preincubation with 25  $\mu\text{mol/L}$  of canrenone resulted in a marked reduction of the  $[\text{Ca}^{2+}]_i$  and of cell contraction.

#### Measurement of Aldosterone Levels in Activated Human Hepatic Stellate Cell Supernatants

Recent studies have indicated that the aldosterone synthase gene *CYP11B2* is expressed in rat HSC, and this expression is upregulated after chronic liver injury.<sup>42</sup> We therefore measured aldosterone levels in the supernatant of different preparations of activated human HSC to evaluate whether some of the observed effects of canrenone are due to a true inhibition of aldosterone actions. In all the samples tested—nonconcentrated or 2 $\times$  and 4 $\times$  concentrated—aldosterone levels were always below the detection limit of the assay (i.e., 0.007 nmol/L), thus indicating that the observed effects of

canrenone in human HSC are likely independent of its antialdosterone action.

#### Discussion

The results of this study indicate that canrenone, an aldosterone antagonist extensively used as a diuretic agent in the treatment of cirrhotic patients with ascites, is able to inhibit growth factor-induced profibrogenic actions of activated human HSC, including cell proliferation, cell motility, and de novo synthesis of ECM components. It is important to note that canrenone exerts these effects independently of its action as an aldosterone antagonist.

In the dose range 1–10  $\mu\text{mol/L}$ , compatible with the concentrations reached by the drug in the serum after oral administration,<sup>43-46</sup> canrenone is able to inhibit cell growth and chemotaxis induced by PDGF without affecting basal cell proliferation and motility. To elucidate which step(s) of PDGF signaling are affected by canrenone, the effects of this drug on the downstream pathways induced by this growth factor were investigated. Preincubation with canrenone did not affect early signaling events, including PDGF- $\beta$  receptor phosphorylation or the phosphorylation of PLC- $\gamma$ , a molecule physically associated with the PDGF receptor. Although the activation of ERK has been shown to be necessary for the mitogenic effect of PDGF,<sup>28,47</sup> the inhibitory effect of canrenone on PDGF-induced mitogenesis and chemotaxis is not exerted through an interference with the activity of this kinase, as also confirmed by the absence of

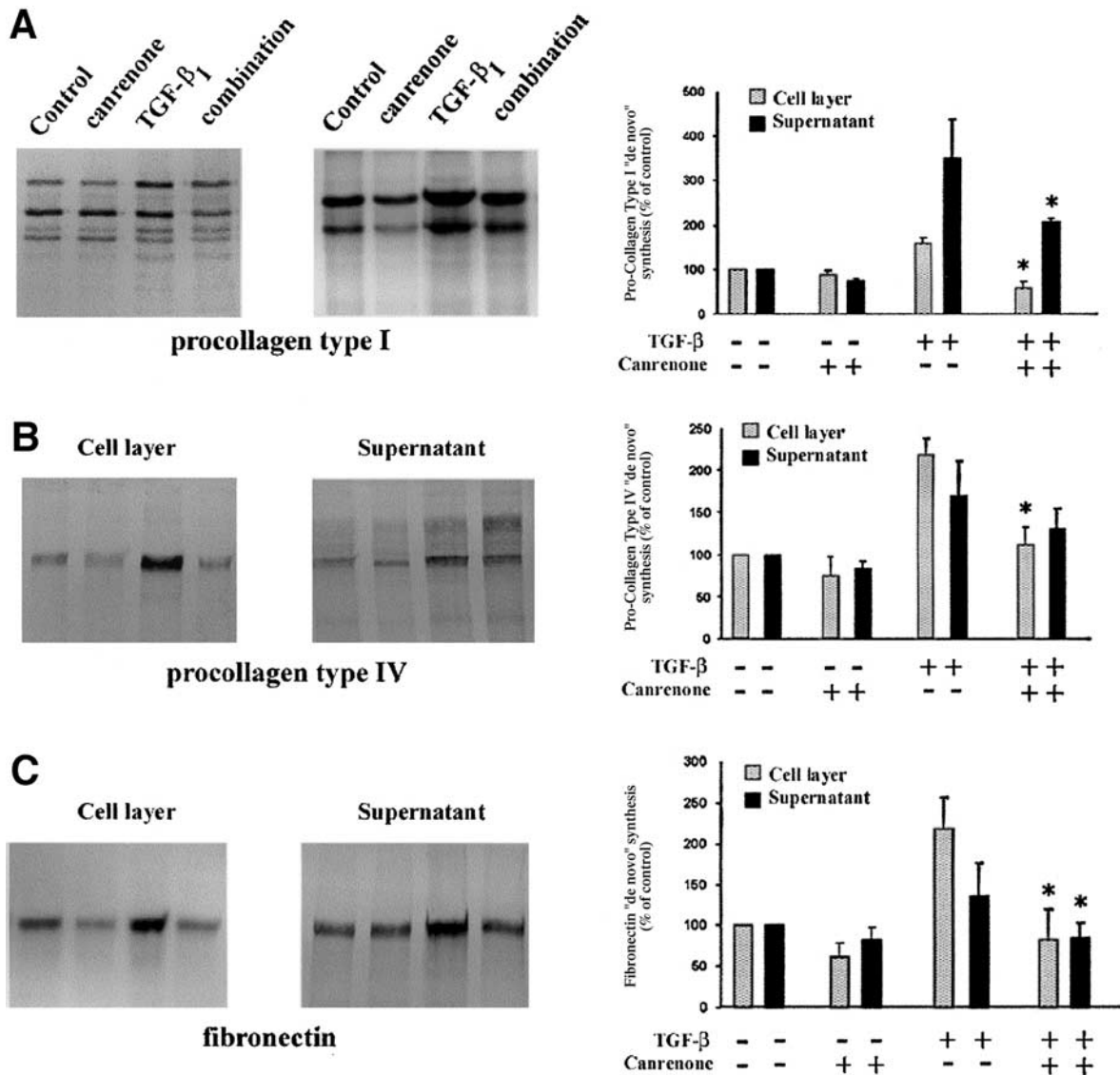


**Figure 12.** Effect of canrenone on the de novo synthesis of different ECM components by activated human HSC. De novo synthesis of procollagen type I (A), procollagen type IV (B), and fibronectin (C) was determined in human HSC supernatants and cell layers by metabolic labeling and immunoprecipitation, as described in Materials and Methods. Activated human HSC were grown to subconfluence in 35-mm Petri dishes in complete culture medium. Cells were washed once with SFIF medium and incubated 24 hours with SFIF medium before treatment with canrenone, TGF- $\beta$ 1, or both. Different conditions were investigated: 1 group of HSC was treated with 25  $\mu$ mol/L of canrenone, and another group was exposed to 1 ng/mL of TGF- $\beta$ 1, whereas a third group was treated with canrenone for 1 hour, followed by an incubation with TGF- $\beta$ 1 for 24 hours. De novo protein synthesis of exposed cells was compared with that of nontreated cells. The results were quantified by Phosphor Imaging with Molecular Analyst software (Bio-Rad). The ratio of [ $^{35}$ S]methionine/[ $^{35}$ S]cysteine incorporation into the protein of treated cells over control cells was calculated for each condition and expressed as mean  $\pm$  SD. At least 3 independent observations (cells of 3 different cultures) were used to calculate the mean. Blots are relative to a representative experiment for each protein investigated. The results are presented as bar graphs, with the control values normalized at 100. To determine the statistical significance of the difference between control and treated cells, 95% confidence intervals were calculated. The effect was considered statistically significant when 100 (normalized control value) did not belong to the 95% confidence interval of the treated/control ratio.

inhibition of its downstream nuclear target *c-fos*. However, data presented herein indicate that canrenone dose-dependently reduces PDGF-induced activity of PI 3-K, a lipid and protein kinase activated through several different pathways, which has been shown to be necessary for both mitogenesis and chemotaxis induced by PDGF in HSC.<sup>23,28</sup> Remarkably, canrenone not only inhibited PI

3-K activity in PDGF-stimulated HSC, but was effective when added in vitro to the immunobeads of the antiphosphotyrosine immunoprecipitates. These findings indicate that canrenone exerts a direct inhibitory effect on PI 3-K activity and that this effect is independent of upstream PDGF signaling or recruitment of the regulatory p85 subunit by the PDGF receptor.

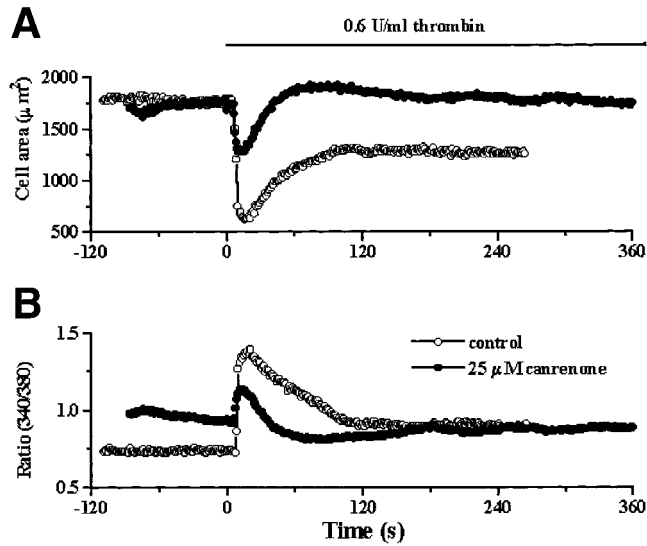


**Figure 13.** Effect of canrenone on thrombin-induced  $[Ca^{2+}]_i$  increase and cell contraction in activated human HSC. Effect of 0.6 U/mL of human thrombin on cell area (A) and  $[Ca^{2+}]_i$  (B) in individual Fura-2 loaded human HSC in the absence (○) or presence (●) of 25  $\mu$ M of canrenone. The time course represents typical examples of the thrombin effect. The horizontal axis indicates time in seconds.

The negative modulation exerted by canrenone on PI 3-K and on its downstream target Akt could be sufficient to explain the interference of this drug with the main biological effects of PDGF. However, because PDGF signaling also involves changes in  $[Ca^{2+}]_i$  and  $[pH]_i$ ,<sup>30,33,34</sup> we next investigated whether canrenone could modulate these events. Experiments investigating the effect of canrenone on PDGF-induced  $[Ca^{2+}]_i$  showed that preincubation with any of the concentrations tested (canrenone 1–50  $\mu$ M) does not affect  $[Ca^{2+}]_i$  changes, in agreement with the lack of effect of canrenone on PLC- $\gamma$  phosphorylation.<sup>35</sup>

Intracellular levels of  $H^+$  are regulated by the NHE, together with other antiporters ( $HCO_3^-/Cl^-$ ,  $Na^+/K^+$ -adenosine triphosphatase). The NHE family includes 6 isoforms (NHE1–NHE6) that function in an electroneutral exchange of intracellular  $H^+$  for extracellular  $Na^+$ . NHE1, the only ubiquitously expressed isoform, is localized at the plasma membrane, where it plays a critical role in  $[pH]_i$  and cell volume homeostasis.<sup>48</sup> In contrast, NHE2–NHE6 have a more limited tissue distribution and are more specialized in function. In addition to its key homeostatic role, NHE1 also functions as a membrane anchor for the actin-based cytoskeleton, independently of its role in ion translocation. It is increasingly evident that through these effects, NHE1 regulates a number of cell functions, including adhesion, cell shape, migration, and proliferation. NHE1 activity is primarily stimulated by changes in intracellular  $H^+$ , such that

reduced  $[pH]_i$  allosterically activates the protein. In addition, its activity is stimulated by several agonists, including growth factors such as PDGF, as also reported in human and rat HSC.<sup>34,49</sup> Inhibition of the activity of the NHE by pretreatment with amiloride inhibits PDGF-induced mitogenesis, thus indicating that changes in  $[pH]_i$  induced by this growth factor are essential for its full biological activity.<sup>33</sup> Along these lines, a role of NHE1, either obligatory or permissive, in the specific cell functions of proliferation, survival, and migration induced by growth factors has recently received the most attention.<sup>48</sup> Our results indicate that, although canrenone is unable to block the activity of the exchanger in response to an acid load, unless used at high dosage (i.e., 50  $\mu$ M/L), it is able to inhibit the antiporter activity stimulated by PDGF. It is therefore conceivable that the effect of canrenone on the biological actions of PDGF is, at least partially, related to the modulation of this important homeostatic system.

Studies performed on different cell types have shown that activation of the NHE1 after stimulation with PDGF is dependent on the activation of different intracellular signaling pathways, including the Ras-mediated ERK cascade<sup>48,50</sup> and Ras-independent signaling cassettes such as the Nck-interacting kinase<sup>51</sup> and PI 3-K.<sup>35</sup> Particularly concerning PI 3-K involvement, activation of NHE1 by PDGF is blocked by preincubation with PI 3-K inhibitors, such as wortmannin, or by inhibition or down-regulation of protein kinase C.<sup>35,52</sup> More precisely, the  $\zeta$  isozyme of protein kinase C has been shown to be a downstream target of phosphatidylinositol 3,4,5-phosphate and to mediate the PI 3-K activation of NHE1.<sup>52,53</sup> Along these lines, the observation that established PI 3-K inhibitors such as wortmannin and LY294002 are able to inhibit PDGF-induced NHE1 activity confirms that PI 3-K is also involved in the regulation of NHE1 in human HSC after stimulation with PDGF. In keeping with this observation, the effect of canrenone on NHE1 activity could be ascribed to its inhibitory effect on PI 3-K activity. At this point, a major issue to be clarified relates to the relative priority of the mechanisms (i.e., inhibition of both PI 3-K and NHE1 activities) responsible for the inhibitory effect of canrenone on PDGF-induced proliferation and migration. Indeed, as previously stated, PI 3-K activity is known to be necessary for both proliferation and migration induced by PDGF in human HSC, whereas the activity of the NHE has been shown to be relevant only for PDGF-induced cell proliferation.<sup>23,28,33</sup> To address this issue, the action of canrenone on PDGF-induced PI 3-K activity and its biological effects was compared with

that of 2 established NHE1 inhibitors, i.e., EIPA and HOE 642. These compounds, which belong to 2 distinct pharmacological classes, are thought to act by competitively inhibiting  $\text{Na}^+$  binding sites at the extracellular cation-binding site of NHE1, with HOE 642 known to be approximately  $10^2$ – $10^3$ -fold more specific than EIPA.<sup>54</sup> It is, however, evident that alternative, not yet elucidated, mechanisms could be responsible for the action of these drugs—amiloride and derivatives in particular.<sup>48</sup> This specific point—the observation that EIPA, at a dosage (10  $\mu\text{mol/L}$ ) usually used to inhibit NHE1 activity, is able to reduce PDGF-induced PI 3-K activity—is of particular interest because it provides evidence for an alternative mechanism of action of this drug. Conversely, the more specific compound HOE 642 is not able to affect PI 3-K. Nevertheless, both EIPA and HOE 642 are able to reduce PDGF-induced mitogenesis and chemotaxis in a dose-dependent fashion.

As previously mentioned, the role of NHE1 is not limited to the regulation of cell volume and  $[\text{pH}]_i$ . Continuously emerging evidence indicates that NHE activity is regulated by the low-molecular-weight guanosine triphosphatase RhoA through the Rho kinase ROCK.<sup>55</sup> In addition, signals from integrin receptors converge with those from heptahelical receptors coupled with  $\text{G}\alpha_{13}$  to activate NHE1 through a RhoA–ROCK cascade.<sup>38,56</sup> In this context, activation of NHE1 provides an inside-out signal to regulate the membrane clustering of integrin receptors and relative downstream events, including assembly of focal adhesions and actin filaments.<sup>38,39,57</sup> In agreement with these data, preincubation of HSC with canrenone, EIPA, or HOE 642 resulted in a dose-dependent inhibition of PDGF-induced FAK phosphorylation, a key event in the cytoskeletal reorganization and cell adhesion modifications necessary for PDGF-induced cell proliferation and migration in human HSC.<sup>40,41</sup> It is therefore conceivable that canrenone, as well as established NHE1 inhibitors, exerts antifibrogenic effects by reducing PDGF mitogenic and chemotactic potential through inhibition of the multifaceted biological actions of NHE1.

Experiments investigating the effect of canrenone on the de novo synthesis of different ECM components induced by TGF- $\beta$  were performed to further substantiate the antifibrogenic potential of this compound. TGF- $\beta$  was used as a well-established inducer of ECM synthesis in rat and human HSC.<sup>24,25</sup> Previous reports obtained in rat HSC have indicated that preincubation with EIPA is able to reduce collagen type I synthesis in cell supernatants induced by oxidative stress,<sup>58</sup> but not that induced by TGF- $\beta$ .<sup>33</sup> However, in these studies,

collagen type I synthesis was assessed by enzyme-linked immunosorbent assay as protein accumulation in cell supernatants. Our data indicate that TGF- $\beta$ -induced de novo synthesis (evaluated by metabolic labeling and immunoprecipitation) of different ECM components—namely, collagen type I, collagen type IV, and fibronectin—is affected by cell preincubation with canrenone. The precise mechanisms of this effect are not clear and would need further evaluation. However, although there is no clear evidence on the role of  $[\text{pH}]_i$  in the regulation of ECM protein synthesis, it is well established that any derangement in the organization of the actin-containing cytoskeleton has implications for the regulation of ECM synthesis.<sup>59,60</sup> Finally, the observation that canrenone may reduce the contractility of activated HSC in response to a strong vasoconstrictor such as thrombin supports the hypothesis, derived from several clinical and experimental studies,<sup>2-5</sup> that antialdosteronic drugs may directly exert beneficial effects on portal pressure.

In conclusion, the in vitro data herein provide evidence that canrenone, the active metabolite of spironolactone, may be active as an antifibrogenic drug and able to reduce the biological effect of profibrogenic agents such as PDGF and TGF- $\beta$ . Canrenone exerts its effects by directly inhibiting the enzymatic activity of PI 3-K and then reducing PDGF-induced activation of NHE1. In addition, the study confirms that any pharmacological intervention able to affect NHE1 activity, either PI 3-K dependent or PI 3-K independent, is able to negatively modulate not only PDGF-induced mitogenesis, but also chemotaxis in human HSC. However, the observation that canrenone, when compared with EIPA and HOE 642, does not affect basal NHE1 activity may represent an important advantage because of the relevant role exerted by NHE1 in biliary secretion.<sup>61,62</sup>

## References

1. Gatta A, Sacerdoti D, Bolognesi M, Merkel C. Portal hypertension: state of the art. *Ital J Gastroenterol Hepatol* 1999;31:326–345.
2. Okumura H, Aramaki T, Katsuta Y, Satomura K, Akaike M, Sekiyama T, Terada H, Ohsuga M, Komeichi H, Tsutsui H. Reduction in hepatic venous pressure gradient as a consequence of volume contraction due to chronic administration of spironolactone in patients with cirrhosis and no ascites. *Am J Gastroenterol* 1991;86:46–52.
3. Nevens F, Lijnen P, VanBilloen H, Fevery J. The effect of long-term treatment with spironolactone on variceal pressure in patients with portal hypertension without ascites. *Hepatology* 1996;23:1047–1052.
4. Garcia-Pagàn JC, Salmeron JM, Feu F, Luca A, Gines P, Pizcueta P, Claria J, Piera C, Arroyo V, Bosch J, Rodés J. Effects of low-sodium diet and spironolactone on portal pressure in patients with compensated cirrhosis. *Hepatology* 1994;19:1095–1099.
5. La Villa G, Barletta G, Romanelli RG, Laffi G, Del Bene R, Vizzutti F, Pantaleo P, Mazzocchi V, Gentilini P. Cardiovascular effects of



- canrenone in patients with preascitic cirrhosis. *Hepatology* 2002; 35:1441–1448.
6. Sorrentino R, Autore G, Cirino G, d'Emmanuele de Villa Bianca R, Calignano A, Vanasia M, Alfieri C, Sorrentino L, Pinto A. Effect of spironolactone and its metabolites on contractile property of isolated rat aorta rings. *J Cardiovasc Pharmacol* 2000;36:230–235.
  7. Cargnelli G, Trevisi L, Debetto P, Luciani S, Bova S. Effects of canrenone on aorta and right ventricle of the rat. *J Cardiovasc Pharmacol* 2001;37:540–547.
  8. Ngarmukos C, Grekin RJ. Nontraditional aspects of aldosterone physiology. *Am J Physiol Endocrinol Metab* 2001;281:E1122–E1127.
  9. Brilla CG, Maisch B. Regulation of the structural remodeling of the myocardium: from hypertrophy to heart failure. *Eur Heart J* 1994; 15:45–52.
  10. Chapman D, Weber KT, Eghbali M. Regulation of fibrillar collagen types I and III and basement membrane type IV collagen gene expression in pressure overloaded rat myocardium. *Circ Res* 1990;67:787–794.
  11. Fullerton MJ, Funder JW. Aldosterone and cardiac fibrosis: *in vitro* studies. *Cardiovasc Res* 1994;28:1863–1867.
  12. Kohler E, Bertschin S, Woodtli T, Resink T, Erne P. Does aldosterone-induced cardiac fibrosis involve direct effects on cardiac fibroblasts? *J Vasc Res* 1996;33:315–326.
  13. Rombouts K, Wielant A, Hellemans K, Schuppan D, Geerts A. Influence of aldosterone on collagen synthesis and proliferation of rat cardiac fibroblasts. *Br J Pharmacol* 2001;134:224–232.
  14. Rombouts K, Niki T, Wielant A, Hellemans K, Schuppan D, Kormoss N, Geerts A. Effect of aldosterone on collagen steady state levels in primary and subcultured rat hepatic stellate cells. *J Hepatol* 2001;34:230–238.
  15. Pinzani M, Gentilini P. Biology of the hepatic stellate cells and its possible relevance in the pathogenesis of portal hypertension in cirrhosis. *Semin Liver Dis* 1999;19:397–410.
  16. Pitt B, Zannad F, Remme WJ, Cody R, Castaigne A, Perez A, Palensky J, Wittes J. The effect of spironolactone on morbidity and mortality in patients with severe heart failure. Randomized Aldactone Evaluation Study Investigators. *N Engl J Med* 1999; 341:709–717.
  17. Funder J. Mineralocorticoids and cardiac fibrosis: the decade in review. *Clin Exp Pharmacol Physiol* 2001;28:1002–1006.
  18. Lacolley P, Safar ME, Lucet B, Ledudal K, Labat C, Benetos A. Prevention of aortic and cardiac fibrosis by spironolactone in old normotensive rats. *J Am Coll Cardiol* 2001;37:662–667.
  19. Oberti F, Pilette C, Rifflet H, Maiga MY, Moreau A, Gallois Y, Girault A, le Bouil A, Le Jeune JJ, Saumet JL, Feldmann G, Cales P. Effects of simvastatin, pentoxifylline and spironolactone on hepatic fibrosis and portal hypertension in rats with bile duct ligation. *J Hepatol* 1997;26:1363–1371.
  20. Oberti F, Rifflet H, Maiga MY, Pilette C, Gallois Y, Douay O, Le Jeune JJ, Saumet JL, Cales P. Prevention of portal hypertension by propranolol and spironolactone in rats with bile duct ligation. *J Hepatol* 1997;26:167–173.
  21. Yang X, Li X, Wu P, Meng Y, Li S, Lai W. CYP11B2 expression in rat liver and the effect of spironolactone on hepatic fibrogenesis. *Horm Res* 2000;53:288–293.
  22. Pinzani M, Gesualdo L, Sabbah GM, Abboud HE. Effects of platelet-derived growth factor and other polypeptide mitogens on DNA synthesis and growth of cultured liver fat-storing cells. *J Clin Invest* 1989;84:1786–1793.
  23. Marra F, Gentilini A, Pinzani M, Ghosh Choudhury G, Parola M, Herbst H, Laffi G, Abboud HE, Gentilini P. Phosphatidylinositol 3-kinase is required for platelet-derived growth factor's action on hepatic stellate cells. *Gastroenterology* 1997;112:1297–1306.
  24. Casini A, Pinzani M, Milani S, Grappone C, Galli G, Jezequel AM, Schuppan D, Rotella CM, Surrenti C. Regulation of extracellular matrix synthesis by transforming growth factor-beta1 in human fat-storing cells. *Gastroenterology* 1993;105:245–253.
  25. Weiner FR, Giambone MA, Czaja MJ, Shah A, Annoni G, Takahashi S, Eghbali M, Zern MA. Ito-cell gene expression and collagen regulation. *Hepatology* 1990;11:111–117.
  26. Pinzani M, Failli P, Ruocco C, Casini A, Milani S, Baldi E, Giotti A, Gentilini P. Fat-storing cells as liver-specific pericytes: spatial dynamics of agonist-stimulated intracellular calcium transients. *J Clin Invest* 1992;90:642–646.
  27. Pinzani M, Gentilini A, Caligiuri A, De Franco R, Pellegrini G, Milani S, Marra F, Gentilini P. Transforming growth factor- $\beta$ 1 regulates platelet-derived growth factor receptor  $\beta$  subunit in human liver fat-storing cells. *Hepatology* 1995;21:232–239.
  28. Marra F, Pinzani M, De Franco R, Laffi G, Gentilini P. Involvement of phosphatidylinositol 3-kinase in action of extracellular signal-regulated kinase by PDGF in hepatic stellate cells. *FEBS Lett* 1995;376:141–145.
  29. Sandirasegarane L, Charles R, Bourbon N, Kester M. NO regulates PDGF-induced activation of PKB but not ERK in A7r5 cells: implications for vascular growth arrest. *Am J Physiol Cell Physiol* 2000;279:C225–C235.
  30. Failli P, Ruocco C, De Franco R, Caligiuri A, Gentilini A, Gentilini P, Giotti A, Pinzani M. Induction of mitogenesis by platelet-derived growth factor in human liver fat-storing cells is dependent upon extracellular calcium influx. *Am J Physiol Cell Physiol* 1995;269: C1133–C1139.
  31. Niki T, Schuppan D, De Bleser PJ, Vrijsen R, Pipeleers Marichal M, Beyaert R, Wisse E, Geerts A. Dexamethasone alters messenger RNA levels but not synthesis of collagens, fibronectin, or laminin by cultured rat fat-storing cells. *Hepatology* 1996;23: 1673–1681.
  32. Schuppan D, Dumont JM, Kim KY, Hennings G, Hahn EG. Serum concentration of the aminoterminal procollagen type III peptide in the rat reflects early formation of connective tissue in experimental liver cirrhosis. *J Hepatol* 1986;3:27–37.
  33. Benedetti A, Di Sario A, Casini A, Ridolfi F, Bendia E, Pignini P, Tonnini C, D'Ambrosio L, Feliciangeli G, Macarri G, Svegliati-Baroni G. Inhibition of the  $\text{Na}^+/\text{H}^+$  exchanger reduces rat hepatic stellate cell activity and liver fibrosis: an *in vitro* and *in vivo* study. *Gastroenterology* 2001;120:545–556.
  34. Di Sario A, Svegliati Baroni G, Bendia E, Ridolfi F, Saccomanno S, Ugili L, Trozzi L, Marzoni M, Jezequel AM, Macarri G, Benedetti A. Intracellular pH regulation and  $\text{Na}^+/\text{H}^+$  exchange activity in human hepatic stellate cells: effect of platelet-derived growth factor, insulin-like growth factor 1 and insulin. *J Hepatol* 2001;34: 378–385.
  35. Ma YH, Reusch HP, Wilson E, Escobedo JA, Fantl WJ, Williams LT, Ives HE. Activation of  $\text{Na}^+/\text{H}^+$  exchange by platelet-derived growth factor involves phosphatidylinositol 3'-kinase and phospholipase C gamma. *J Biol Chem* 1994;269:30734–30739.
  36. Lee-Kwon W, Johns DC, Cha B, Cavet M, Park J, Tschlis P, Donowitz M. Constitutively active phosphatidylinositol 3-kinase and AKT are sufficient to stimulate the epithelial  $\text{Na}^+/\text{H}^+$  exchanger 3. *J Biol Chem* 2001;276:31296–31304.
  37. Janecki AJ, Janecki M, Akhter S, Donowitz M. Basic fibroblast growth factor stimulates surface expression and activity of  $\text{Na}^+/\text{H}^+$  exchanger NHE3 via mechanism involving phosphatidylinositol 3-kinase. *J Biol Chem* 2000;275:8133–8142.
  38. Tominaga T, Barber DL. Na-H exchange acts downstream of RhoA to regulate integrin-induced cell adhesion and spreading. *Mol Biol Cell* 1998;9:2287–2303.
  39. Belusa R, Aizman O, Andersson RM, Aperia A. Changes in  $\text{Na}^+$ -K $^+$ -ATPase activity influence cell attachment to fibronectin. *Am J Physiol Cell Physiol* 2002;282:C302–C309.
  40. Carloni V, Romanelli RG, Pinzani M, Laffi G, Gentilini P. Focal adhesion kinase and phospholipase C  $\gamma$  involvement in cell

- adhesion and migration of human hepatic stellate cells. *Gastroenterology* 1997;112:522–531.
41. Carloni V, Pinzani M, Giusti S, Romanelli RG, Parola M, Bellomo G, Failli P, Hamilton AD, Sebti SM, Laffi G, Gentilini P. Tyrosine phosphorylation of focal adhesion kinase by PDGF is dependent on ras in human hepatic stellate cells. *Hepatology* 2000;31:131–140.
  42. Li X, Yang X, Wu P, Meng Y, Li S, Lai W. Gene-CYP11B2 expression in rat liver in hepatic fibrogenesis induced by CCl<sub>4</sub>. *Chin Med J* 2001;114:64–68.
  43. Overdiek HW, Hermens WA, Merkus FW. New insights into the pharmacokinetics of spironolactone. *Clin Pharmacol Ther* 1985;38:469–474.
  44. Kojima K, Yamamoto K, Fujioka H, Kaneko H. Pharmacokinetics of spironolactone and potassium canrenoate in humans. *J Pharmacobiodyn* 1985;8:161–166.
  45. Ho PC, Bourne DW, Triggs EJ, Smithurst BA. Comparison of plasma levels of canrenone and metabolites after base hydrolysis in young and elderly subjects following single and multiple doses of spironolactone. *Eur J Clin Pharmacol* 1984;27:435–439.
  46. Merkus FW, Overdiek JW, Cilissen J, Zuidema J. Pharmacokinetics of spironolactone after a single dose: evaluation of the true canrenone serum concentrations during 24 hours. *Clin Exp Hypertens A* 1983;5:239–248.
  47. Marra F, Arrighi MC, Fazi M, Caligiuri A, Pinzani M, Romanelli RG, Efsen E, Laffi G, Gentilini P. Extracellular signal-regulated kinase activation differentially regulates platelet-derived growth factor's actions in hepatic stellate cells, and is induced by *in vivo* liver injury in the rat. *Hepatology* 1999;30:951–958.
  48. Putney LK, Denker SP, Barber DL. The changing face of the Na<sup>+</sup>/H<sup>+</sup> exchanger, NHE1: structure, regulation, and cellular actions. *Annu Rev Pharmacol Toxicol* 2002;42:527–552.
  49. Di Sario A, Bendia E, Svegliati Baroni G, Ridolfi F, Bolognini L, Feliciangeli G, Jezequel AM, Orlandi F, Benedetti A. Intracellular pathways mediating Na<sup>+</sup>/H<sup>+</sup> exchange activation by platelet-derived growth factor in rat hepatic stellate cells. *Gastroenterology* 1999;116:1155–1166.
  50. Bianchini L, L'Allemain G, Pouyssegur J. The p42/p44 mitogen-activated protein kinase cascade is determinant in mediating activation of the Na<sup>+</sup>/H<sup>+</sup> exchanger (NHE1 isoform) in response to growth factors. *J Biol Chem* 1997;272:271–279.
  51. Yan W, Nehrke K, Choi J, Barber DL. The Nck-interacting kinase (NIK) phosphorylates the Na<sup>+</sup>/H<sup>+</sup> exchanger NHE1 and regulates NHE1 activation by platelet-derived growth factor. *J Biol Chem* 2001;276:31349–31356.
  52. Sauvage M, Maziere P, Fathallah H, Giraud F. Insulin stimulates NHE1 activity by sequential activation of phosphatidylinositol 3-kinase and protein kinase C zeta in human erythrocytes. *Eur J Biochem* 2000;267:955–962.
  53. Nakanishi H, Brewer KA, Exton JH. Activation of the zeta isozyme of protein kinase C by phosphatidylinositol 3,4,5-trisphosphate. *J Biol Chem* 1993;268:13–16.
  54. Counillon L, Scholz W, Lang HJ, Pouyssegur J. Pharmacological characterization of stably transfected Na<sup>+</sup>/H<sup>+</sup> antiporter isoforms using amiloride analogs and a new inhibitor exhibiting anti-ischemic properties. *Mol Pharmacol* 1993;44:1041–1045.
  55. Hooley R, Yu CY, Symons M, Barber DL. G alpha 13 stimulates Na<sup>+</sup>/H<sup>+</sup> exchange through distinct Cdc42-dependent and RhoA-dependent pathways. *J Biol Chem* 1996;271:6152–6158.
  56. Tominaga T, Ishizaki T, Narumiya S, Barber DL. p160ROCK mediates RhoA activation of Na-H exchange. *EMBO J* 1998;17:4712–4722.
  57. Denker SP, Huang DC, Orlowski J, Furthmayr H, Barber DL. Direct binding of the Na-H exchanger NHE1 to ERM proteins regulates the cortical cytoskeleton and cell shape independently of H(+) translocation. *Mol Cell* 2000;6:1425–1436.
  58. Svegliati-Baroni G, Di Sario A, Casini A, Ferretti G, D'Ambrosio L, Ridolfi F, Bolognini L, Salzano R, Orlandi F, Benedetti A. The Na<sup>+</sup>/H<sup>+</sup> exchanger modulates the fibrogenic effect of oxidative stress in rat hepatic stellate cells. *J Hepatol* 1999;30:868–875.
  59. Dhawan J, Farmer SR. Induction of collagen synthesis in response to adhesion and TGF beta is dependent on the actin-containing cytoskeleton. *Adv Exp Med Biol* 1994;358:159–168.
  60. Varedi M, Ghahary A, Scott PG, Tredget EE. Cytoskeleton regulates expression of genes for transforming growth factor-beta 1 and extracellular matrix proteins in dermal fibroblasts. *J Cell Physiol* 1997;172:192–199.
  61. St-Pierre MV, Kullak-Ublick GA, Hagenbuch B, Meier PJ. Transport of bile acids in hepatic and non-hepatic tissues. *J Exp Biol* 2001;204:1673–1686.
  62. Hubner C, Stremmel W, Elsing C. Sodium, hydrogen exchange type 1 and bile ductular secretory activity in the guinea pig. *Hepatology* 2000;31:562–571.

---

Received June 6, 2002. Accepted October 31, 2002.

Address requests for reprints to: Massimo Pinzani, M.D., Ph.D., Dipartimento di Medicina Interna, Università di Firenze, Viale G.B. Morgagni, 85, I-50134 Firenze, Italy. e-mail: m.pinzani@dmi.unifi.it; fax: (39) 055-417123.

Supported by grants from the Italian MURST (project "Cellular and Molecular Biology of Hepatic Fibrogenesis"), from the Università di Firenze, from Banco di Roma, Rome, Italy, and from Gienne Pharma S.p.A, Milan, Italy.